Transcriptome Analysis to Identify the Potential Role of Long non-coding RNAs in Enteric Glial Cells under Hyperglycemia

Xuping Zhu
Department of Endocrinology, The Affiliated Wuxi People's Hospital of Nanjing Medical University, Nanjing Medical University

Yanyu Li
Department of Endocrinology, The Affiliated Wuxi People's Hospital of Nanjing Medical University, Nanjing Medical University

Xue Zhu
Laboratory of Nuclear Medicine, Jiangsu Key Laboratory of Molecular Nuclear Medicine, Jiangsu Institute of Nuclear Medicine

Yanmin Jiang
Department of Endocrinology, The Affiliated Wuxi People's Hospital of Nanjing Medical University, Nanjing Medical University

Xiaowei Zhu
Department of Endocrinology, The Affiliated Wuxi People's Hospital of Nanjing Medical University, Nanjing Medical University

Xiang Xu
Department of Endocrinology, The Affiliated Wuxi People's Hospital of Nanjing Medical University, Nanjing Medical University

Chao Liu
Department of Endocrinology, The Affiliated Wuxi People's Hospital of Nanjing Medical University, Nanjing Medical University

Chengming Ni
Department of Endocrinology, The Affiliated Wuxi People's Hospital of Nanjing Medical University, Nanjing Medical University

Lan Xu (xulan126@126.com)
Department of Endocrinology, The Affiliated Wuxi People's Hospital of Nanjing Medical University, Nanjing Medical University

Ke Wang (wangke@jsinm.org)
Laboratory of Nuclear Medicine, Jiangsu Key Laboratory of Molecular Nuclear Medicine, Jiangsu Institute of Nuclear Medicine

Research Article

Keywords: Diabetic gastrointestinal autonomic dysfunction, LncRNA, Enteric glial cell, Hyperglycemia

Posted Date: December 9th, 2020

DOI: https://doi.org/10.21203/rs.3.rs-118235/v1

Abstract

Background

Long non-coding RNAs (lncRNAs) are important mediators in the pathogenesis of diabetic gastrointestinal autonomic neuropathy, which has just been reported to have a relation to enteric glial cells (EGCs). However, the role of lncRNAs in the pathogenesis of diabetic gastrointestinal autonomic neuropathy, especially EGCs-related gastrointestinal dysfunction, has never been reported.

Methods

RNA sequencing technology (RNA-Seq) was used to screen the differential lncRNAs and mRNAs in EGCs under hyperglycemia (300 mmol L^{-1} high glucose).

Results

Totally 4678 differentially expressed lncRNAs (DE lncRNAs) and 6244 differentially expressed mRNAs (DE mRNAs) were obtained. GO enrichment analysis and KEGG pathway analysis showed significant differences. 2910 and 1549 co-expressed mRNAs were respectively expressed in up-regulated and down-regulated DE lncRNA target genes. Several up- or down-regulated lncRNAs were at the key junction points of the regulatory network. Protein-protein interaction networks showed highly connected clusters were TP53, AKT1, Casp9, Casp8, Casp3, TNF, etc, which are known closely related to apoptosis. FLRT3, Fras1, and other related target genes, which revealed the potential function of lncRNAs, may be important targets for differential lncRNAs to regulate the apoptosis of glial cells induced by hyperglycemia.

Conclusion

In this study, the involvement of lncRNAs in EGCs under hyperglycemia was analyzed using transcriptome analysis.

Introduction

Diabetes Mellitus (DM) is one of the most serious chronic diseases in the world and a continuous rise in DM prevalence is expected. According to World Health Organization statistics, > 422 million adults globally were suffering from DM since 2014[1] and 8.8% of the global adults have been diagnosed with diabetes[2]. Diabetic gastrointestinal autonomic dysfunction is a common complication of DM, which occurs in 50–55% of diabetic patients. Diabetic gastrointestinal autonomic dysfunction shows various gastrointestinal symptoms, such as abdominal pain or discomfort, abdominal distention, nausea, vomiting, diarrhea, constipation, etc[3–5]. Intestinal sensory and motile gastric dysfunction is the main

cause of diabetic gastrointestinal autonomic neuropathy, which is closely related to the damage of the enteric nervous system (ENS) in diabetic patients[6, 7].

ENS is mainly composed of enteric glial cells (EGCs), enteric nerve cells (ENCs), and interstitial cells of Cajal (ICC), which controls diverse aspects of digestive physiology, including intestinal peristalsis, secretion, and blood flow[8]. As the most important component of ENS, ENCs are usually considered as the cause of the occurrence and development of gastrointestinal diseases[5, 9, 10]. However, as another major component of ENS, the function of EGCs in gastrointestinal physiology and pathophysiology has just been noticed recently. EGCs contribute to supporting and nourishing ENCs[11], regulating gastrointestinal movement[12], and participating in the formation of a gastrointestinal barrier[11, 13–15]. As well, EGCs display neurotransmitter, immune and homeostatic functions[9, 16]. Neunlist et al. found that EGCs participate in the intestinal epithelial barrier (EB) function by regulating the expression of tight junction proteins and affecting cell bypass permeability and epithelial cell proliferation[17]. Gulbransen et al. found that EGCs can recognize the activity of adjacent synaptic pathways and selectively responds to sympathetic activation[18]. They can also protect ENCs from injury by releasing glial cell-derived neurotrophic factor (GDNF) or reduced glutathione Oxidative damage promotes synaptic communication of intestinal neurons[19, 20]. Until now, the detailed function of EGCs in diabetic gastrointestinal autonomic neuropathy has never been clearly identified.

Long non-coding RNAs (lncRNAs) are transcripts with a length of more than 200 nucleotides and a lack of protein-coding ability[21]. In the past 10 years, lncRNAs have been considered as the key molecules to regulate cell proliferation, cell differentiation, and tumor metastasis[21]. Increasing evidence has shown that lncRNAs play an important role in the pathogenesis of diabetes and its complications[22, 23]. Wang et al. have found abnormal expression of lncRNAs in Chinese patients with type 2 diabetes, and further revealed that abnormal expression of lncRNAs played an important role in the pathogenesis of diabetes by regulating inflammation and insulin resistance[24]. LncRNA-MALAT1 has been reported to be involved in the pathogenesis of diabetes and its complications through a variety of signaling pathways, including SREBP-1c, p38 MAPK pathway related to endoplasmic reticulum stress, and the release of inflammatory cytokines TNF - α, IL-1 β and IL-6[25, 26]. However, the role of lncRNAs in the pathogenesis of diabetic gastrointestinal autonomic neuropathy, especially EGCs-related gastrointestinal dysfunction, has never been reported.

In this study, RNA sequencing was used to analyze transcriptome change of lncRNAs and mRNAs in hyperglycemia-treated EGCs, which would provide a new perspective and lay the foundation for the further function study of lncRNAs and mRNAs in diabetic gastrointestinal autonomic neuropathy. The data may open novel therapeutic approaches for diabetic gastrointestinal autonomic neuropathy.

Materials And Methods

Cell line and culture

EGCs (EGC/PK060399egfr; ATCC® CRL-2690™) were purchased from ATCC (Manassas, VA, USA) and cultured in DMEM medium (Gibco, Grand Island, NY, USA)) supplemented with 10% (v/v) heat-inactivated fetal bovine serum (Biological Industries, Kibbutz Beit Haemek, Israel). The original glucose concentration of the DMEM medium to cultivate EGCs is 25 mM (mmol L^{-1}). We used D- (+) -Glucose (Sigma, St. Louis, MO, USA) to modulate hyperglycemia concentration and D- (+) -Mannitol (Sangon Biotech, Shanghai, China) to modulate hypertonic concentration[27, 28].

Cell viability assay

EGCs were seeded into 96-well plates at 10^4 cells per well and allowed to adhere overnight. After D-(+)-Glucose or D-(+)-Mannitol treatment, 10 μL of MTT (Beyotime, Nantong, China) solution (5 mg/mL) was added to each well, and incubated at 37°C for 4 h in the dark. Following removal of the MTT solution and addition of 150 μL dimethyl sulfoxide (Beyotime, Nantong, China) to dissolve the formazan crystals, the absorbance at 570 nm was measured with a microplate reader[29, 30]. Cell viability was determined by calculating the absorbance ratio of treated cells to control cells.

Cell apoptosis assay

In situ detection of DNA fragments by terminal deoxyribonucleotide transferase (TdT)-mediated dUTP nick end labeling (TUNEL) was performed using the one-step TUNEL apoptosis assay kit (Beyotime, Nantong, China). After D-(+)-Glucose treatment, cells were rinsed with PBS, then permeabilized by 0.1% Triton X-100. After washed with PBS, cells were added with 50 μl of TUNEL reaction mixture, then incubated for 1 h at 37° C in the dark. Confocal Laser Scanning Microscope by using 530 nm emission and the images were captured by image analysis software[31, 32]. The cells with red fluorescence were defined as apoptotic cells.

RNA quantification and qualification

RNA degradation and contamination were monitored on 1% agarose gels. RNA purity was checked using the NanoPhotometer® spectrophotometer (IMPLEN, CA, USA). RNA concentration was measured using the Qubit® RNA Assay Kit in Qubit® 2.0 Fluorometer (Life Technologies, CA, USA). RNA integrity was assessed using the RNA Nano 6000 Assay Kit of the Bioanalyzer 2100 system (Agilent Technologies, CA, USA).

Library preparation for transcriptome sequencing

A total amount of 3 μg RNA per sample was used as input material for the RNA sample preparations. Sequencing libraries were generated using NEBNext® UltraTM RNA Library Prep Kit for Illumina® (New England Biolabs, Ipswich, MA, USA) following manufacturer's recommendations and index codes were added to attribute sequences to each sample. Briefly, mRNA was purified from total RNA using poly-T oligo-attached magnetic beads. Fragmentation was carried out using divalent cations under elevated temperature in NEBNext First Strand Synthesis Reaction Buffer(5X). The first-strand cDNA was

synthesized using random hexamer primer and M-MuLV Reverse Transcriptase (RNase H). Second strand cDNA synthesis was subsequently performed using DNA Polymerase I and RNase H. Remaining overhangs were converted into blunt ends via exonuclease/polymerase activities. After the adenylation of 3’ ends of DNA fragments, NEBNext Adaptor with a hairpin loop structure was ligated to prepare for hybridization. In order to select cDNA fragments of preferentially 150~200 bp in length, the library fragments were purified with the AMPure XP system (Beckman Coulter, Indianapolis, IN, USA). Then 3 μl USER Enzyme (New England Biolabs, Ipswich, MA, USA) was used with size-selected, adaptor-ligated cDNA at 37°C for 15 min followed by 5 min at 95 °C before PCR. Then PCR was performed with Phusion High-Fidelity DNA polymerase, Universal PCR primers and Index (X) Primer. At last, PCR products were purified (AMPure XP system), and library quality was assessed on the Agilent Bioanalyzer 2100 system[33].

Clustering and sequencing

The clustering of the index-coded samples was performed on a cBot Cluster Generation System using TruSeq PE Cluster Kit v3-cBot-HS (Illumina, San Diego, California, USA) according to the manufacturer’s instructions[34]. After cluster generation, the library preparations were sequenced on an Illumina Hiseq platform and 125 bp/150 bp paired-end reads were generated.

Quality control

Raw data (raw reads) of FASTQ format were firstly processed through in-house Perl scripts. In this step, clean data (clean reads) were obtained by removing reads containing adapter, reads containing ploy-N and low-quality reads from raw data. All clean reads were aligned to the reference genome and gene model annotation databases using bowtie2 (v2.2.8) and HISAT2 (v2.0.4)[35], respectively. The aligned reads from all samples were assembled by StringTie (v1.3.1)[34]. At the same time, Q20, Q30 and GC content the clean data were calculated. All the downstream analyses were based on clean data with high quality.

Reads mapping to the reference genome

Reference genome and gene model annotation files were downloaded from the genome website directly. The index of the reference genome was built using STAR and paired-end clean reads were aligned to the reference genome using STAR (v2.5.1b)[36]. STAR used the method of Maximal Mappable Prefix (MMP) which can generate a precise mapping result for junction reads.

Quantification of gene expression level

HTSeq (v0.6.0) was used to count the reads numbers mapped to each gene[34]. And then FPKM (fragments per kilobase of transcript per million fragments mapped) of each gene was calculated based on the length of the gene and reads count mapped to this gene. FPKM, expected number of Fragments Per Kilobase of transcript sequence per Millions of base pairs sequenced, considers the effect of

sequencing depth and gene length for the reads count at the same time, and is currently the most used method for estimating gene expression levels.

Differential expression analysis

Before differential gene expression analysis, for each sequenced library, the read counts were adjusted by the edgeR program package through one scaling normalized factor. Differential expression analysis of two conditions was performed using the edgeR R package (3.12.1). The P values were adjusted using the Benjamini & Hochberg method[37]. Corrected P-value of 0.05 and absolute foldchange of 2 was set as the threshold for significantly differential expression. Heat map clustering analysis of all differentially expressed lncRNAs and mRNAs was calculated using the Heatmaps R package.

GO and KEGG enrichment analysis

Gene Ontology (GO) enrichment analysis was implemented by the cluster profiler R package, in which gene length bias was corrected (http://geneontology.org/). GO terms with corrected P-value less than 0.05 were considered significantly enriched by differential expressed target genes. KEGG is a database resource for understanding high-level functions and utilities of the biological system, such as the cell, the organism and the ecosystem, from molecular-level information, especially large-scale molecular datasets generated by genome sequencing and other high-throughput experimental technologies (http://www.genome.jp/kegg/). We used the cluster profiler R package to test the statistical enrichment of differentially expressed target genes in KEGG pathways.

mRNA-lncRNA-miRNA co-expression network analysis

A lncRNA-miRNA-mRNA co-expression network was constructed based on the differentially expressed lncRNAs, mRNAs and miRNAs[38], and the interactions in the network were analyzed using Cytoscape software (http://www.cytoscape.org/). Different colors represent different types of RNA.

Protein-Protein interaction network (PPI)

Protein-protein interaction network between differentially expressed lncRNA target genes was analyzed by the STRING database (https://string-db.org/), and further visualized with Cytoscape software (http://www.cytoscape.org/)[39].

Prediction and functional enrichment analysis of lncRNA target genes

To reveal the potential function of lncRNAs, their target genes were predicted in Cis. For Cis role, it refers to the action of lncRNA on neighboring target genes. In this study, the coding genes from 100 kb upstream and downstream of a lncRNA were searched.

Real-time quantitative PCR (RT-qPCR)

To validate the RNA-Seq results, cDNA was synthesized by reverse transcription using 1μg of the original RNA sample as described previously. RNAs were reverse-transcribed using the PrimeScript™RT reagent Kit (Perfect Real Time) (TAKARA, Dalian, China) according to the manufacturer's instructions. cDNA was analyzed by using TB Green™ Premix Ex Taq™ II (Tli RNaseH Plus) (TAKARA, Dalian, China). GAPDH was chosen as the reference gene. The threshold cycle (CT) value was detected by the 7500 Fast Real-Time PCR system (Applied Biosystems, CA, USA)[40]. The expression levels were computed according to the $2^{-\Delta\Delta Ct}$ method.

Statistical analysis

GraphPad software Prism (5.0) was used for statistical analysis. Differences between the treatment groups were analyzed by one-way ANOVA with Bonferroni's or Dunnett's posttests. A P-value of less than 0.05 was considered significantly enriched.

Results

Hyperglycemia induces cytotoxicity and cell apoptosis in EGCs

To investigate the effect of hyperglycemia on EGCs, cells were cultured with different concentrations of D-(+)-Glucose (0, 50, 100, 200, 300, 400 mM) for 24h. Cell viability determined by the MTT assay was used to measure metabolic activity (intracellular NADH concentration) of the cells. As shown in Figure 1A, G300 (Glucose300) treatment induced the viability of cells from 100.00% ± 8.85% to 74.07% ± 8.71%, thus which was selected as representative concentration. The significance was determined by the ANOVA test (*P□0.05, **P□0.01, ***P□0.001, ****P□0.0001 compared with G0). Then, cell apoptosis was determined by the Tunnel assay. As shown in Figure 1B, G300 obviously induced shrinkage, and the formation of apoptotic bodies was observed, while the apoptosis of M300 was significantly less than that of G300, which meant that apoptosis was caused by hyperglycemia, not by hypertonic. Tunnel assay showed that typical apoptotic cells were labeled with red fluorescence (marked by the white arrows).

Sequencing data overview in EGCs under hyperglycemia

A total of 104821486 and 116495776 raw reads were produced using the Illumina PE150 platform in G0 and G300 groups. After discarding adaptor sequences and low-quality sequences, 101754234 and 111958252 corresponding clean reads were obtained, and the percentage of clean reads was 97.07% and 96.10% (Table 1). The raw bases, clean bases, and the percentage of Q20, Q30, GC content of the cleaned reads were calculated and shown in Table 2. The percent of reads to genome regions were shown in Figure 2A and the results revealed that most clean reads in the two periods were located in the exonic region, and about 20% of the total clean reads were in the intergenic region of the genome. The percent of the intronic region in G0 and G300 was 16.23% and 9.03%. The transcript length, exon number, and ORF were calculated and shown in Figure 2B. Most of the lncRNA lengths were less than 2500, while mRNAs were distributed between 0 and > 1000. The exons and ORF lengths of lncRNAs and mRNAs also showed similar patterns with length. The exon lengths of lncRNAs were less than 10, while that of mRNA was

between 0 and 30. The ORF length of lncRNAs was less than 500, while most of the exon lengths of mRNAs were evenly distributed between 0-2000. It showed the difference between lncRNAs and mRNAs and it verifies that the predicted novel lncRNAs conformed to the general characteristics.

Table 1 The information of sequencing data.

Sample name	Raw reads	Clean reads	Clean reads ratio
G0	104,821,486	101,754,234	97.07%
G300	116,495,776	111,958,252	96.10%

Table 2 Summary of transcriptome results.

Sample name	Raw bases(G)	Clean bases(G)	Q20(%)	Q30(%)	GC content(%)
G0	15.72	15.26	98.31	94.89	48.94
G300	17.47	16.79	98.4	95.16	52.42

Differential expression of lncRNAs and mRNAs in EGCs under hyperglycemia

The volcano plots were constructed to show the rapid evaluation of differentially expressed lncRNAs and mRNAs as well as their statistical significance (Figure 3A). Each point in the volcano plot represented a lncRNA or an mRNA, and the abscissa represented the logarithm of the fold change (FC) in the expression of RNAs between the 2 groups. Higher absolute values were correlated with larger differences. Down-regulated lncRNAs were represented in green, and up-regulated lncRNAs were shown in red. The black dots represented lncRNAs that were not significantly differentially expressed. Totally 4678 DE lncRNAs and 6244 DE mRNAs were obtained according to the fold change ≥ 2 and padj <0.05. Among these, 3295 DE lncRNAs and 3010 DE mRNAs were up-regulated, and 1383 DE lncRNAs and 3234 DE mRNAs were down-regulated in the G300 group compared to the G0 group. A Heatmap was presented to show the clustering of the DE lncRNAs and mRNAs based on expression (Figure 3B). Red indicated high relative expression, and blue indicated low relative expression. The samples were grouped by hierarchical clustering, and a circus plot was generated to show the location and expression values of the identified lncRNAs and mRNAs in two groups (Figure 3C). The outermost ring indicates the genome, the middle one indicates the mRNAs expression, and the innermost circle showing the lncRNAs expression. In all, according to the transcriptional level, there were significant differences between the two groups.

GO enrichment analysis of DE mRNAs and DE lncRNA target genes

To investigate the probable function of candidate lncRNAs, the nearby coding genes around 100kb up and downstream from the identified lncRNAs, termed as Cis-regulatory function, were searched. Then functional enrichment analysis of the significantly regulated genes was performed based on their relative expression and fold changes. As shown in Figure 4A-B, the top 20 significantly enriched GO terms (padj <0.05) were identified in three parts: Molecular Function (MF), Biological Process (BP), Cellular

Component (CC). Figure 4A showed GO enrichment analysis of differentially expressed genes (DEGs), such as multicellular organismal development (GO:0007275), single-organism process (GO:0044699), and protein binding (GO:0005515), etc. Figure 4B showed GO enrichment analysis of DE lncRNA target genes, such as metabolic process (GO:0008152), protein binding (GO:0005515), organic substance metabolic process (GO:0071704), etc.

KEGG enrichment analysis of DE mRNAs and DE lncRNA target genes

The top 20 enriched KEGG pathways obtained from the DE mRNAs or DE lncRNA target genes were listed in Figure 5A-B (Padj<0.05). The ECM-receptor interaction, Hypertrophic Cardiomyopathy (HCM) and Transcriptional Mis-regulation in cancer were identified in the KEGG pathway analysis as containing the highest rich factor in DE mRNAs (Figure 5A). The Non-small cell lung cancer, estrogen signaling pathway and endometrial cancer were identified in the KEGG pathway analysis as containing the highest rich factor in DE lncRNA target genes (Figure 5B). Apart from the basic cellular activities, other pathways, including MAPK signaling pathway, T cell receptor signaling pathway and Base excision repair, have been proved to be involved in cell metabolism, synthesis, immune response, apoptosis and other important life activities[22, 41]. DE mRNAs and DE lncRNA target mRNAs were shown in the Venn diagrams. 2910 and 1549 co-expressed mRNAs were respectively expressed in up-regulated and down-regulated DE lncRNA target genes (Figure 5C-D).

Then, 19 KEGG pathways related to apoptosis, such as apoptosis, Jak-STAT signaling pathway, PI3K-Akt signaling pathway, NF-kappa B signaling pathway were analyzed. We listed the expression of DE mRNAs and DE lncRNA target genes in each pathway and marked the co-expressed targets (Table 3). Co-expression of DE mRNAs and DE lncRNA target genes in these pathways can be considered as important targets for apoptosis, such as Bcl2, Tp53, Wnt4, TRADD, Bax, TNF, which are widely believed to be involved in apoptosis regulation.

Table 3 The expression of DE mRNAs and DE lncRNA target genes in apoptosis related pathways.

Pathways	RNA	Targets
Apoptosis	lncRNAs Targets	Casp8, Irak1, **Bcl2l1**, Il1a, Akt1, **AC098008.1**, Casp9, **Bcl2**, Prkar2a, Pik3r2, Capn1, Ntrk1, Tnfrsf1a, Il1r1, Map3k14, **Tradd**, Prkacb, **Prkar2b**, Casp6, Bax, Pik3cd, Irak3, **Capn8**, **Faslg**, Pik3ca, **Birc3**, Il3, Ppp3r1, Ripk1, Prkaca, Akt2, **Ngf**, Prkar1a, LOC103689977, Rela, **Cela2a**, Irak4, Csf2rb, Casp3, Bad, Tnf, LOC103694380, Ppp3cc, Birc2, Fadd, Chuk, **Irak2**, Casp7, **Tp53**, Pik3r3, Akt3, Cflar, **Pik3r1**
	mRANs	Ikbkb, Fas, **Tp53**, Nfkbia, **Bcl2l1**, **Tradd**, Ppp3cb, **Capn8**, **Ngf**, **Prkar2b**, **Cela2a**, Pik3r5, **AC098008.1**, **Irak2**, **Bcl2**, LOC100363502, LOC100910021, Myd88, **Birc3**, **Faslg**, **Pik3r1**
MAPK signaling pathway	lncRNAs Targets	**Map3k8**, **Fgf18**, Gna12, Gadd45a, **Pla2g4c**, **Cacnb4**, AABR07003173.1, Map2k7, Cacng2, Tnfrsf1a, Sos2, Crk, Fgf2, Mapk11, Fgf17, Mapk8ip3, Dusp4, Grb2, **Fgf22**,**Pdgfb**, Casp3, **Cacna2d2**, Myc, **Dusp16**, **Ptprr**, Ppp3cc, Jun, Map3k5, Fgfr3, **Rasgrp2**, Max, **Ntf4**, **Tp53**, Akt3, Fgf1, Mapk14, AABR07001516.1, **Il1r2**, Dusp9, **Dusp10**, **Pcbp2**, **Dusp5**, Akt1, **AABR07007642.1**, Mapkapk2, **Rps6ka3**, **Fgfr1**, **Pak2**, **AABR07033324.1**, **Mapt**, **Faslg**, Map2k1, **Hras**, LOC100912585, Map2k5, Stk4, **Cacna1h**, **Ngf**, Ppm1b, Prkaca, Rasa2, **Dusp1**, Rela, Chuk, Hspa5, Cdc42, Sos1, Rap1a, **Atf4**, Map3k12, **Fgf5**, Tab1, Map3k13, Dusp3, **Mapk3**, Il1r1, Prkacb, Cacna2d4, Rps6ka1, Map4k4, Braf, Il1a, Relb, Rps6ka4, **Cacnb3**, Pla2g4d, Map3k6, **Rapgef2**, Ntrk1, **Flna**, **Ptpn7**, Fgf16, Taok2, Ecsit, **Hspa1b**, Raf1, LOC100910771, **LOC100912365**, **Fosl2**, **Pla2g4f**, Ppp3r1, Jund, Akt2, Tnf, **Cacng5**, Fgf23, Mapk9, Rap1b, **Mef2c**, **Prkca**, Fgf21, Nfkb2, Map3k3, Map3k4, **Hspa1l**, Cacna1g, **Mapk10**, Rasgrp1, Map2k4, **Cacna1a**, Rasgrf1, Map3k20, Nr4a1, Arrb2, Dusp2, **Plg**, Ppm1a, Hspa2, **Gadd45g**, **Fgf7**, **Cdc25b**, Map3k14, LOC108348190, Flnc, LOC100910732, LOC102552659, Fos, Nfatc1, Map3k2, Fgf3, **Hspb1**, Rras, Tgfbr2, Dusp6, Fgf8, Fgf6, Gng14, Map4k2, **Gng12**, **Tgfb2**, Dusp8, Cacna1d, LOC103694380, Mapk12, Fgfr4, Daxx, **Map4k3**, **Fgf19**, Fgf4, Cacnb1, Rac2
	mRANs	Ntrk2, **Fgf18**, **Map3k8**, Mapk8, Uxt, Fgfr2, Cacna1c, Mecom, Rasgrp4, **Cacnb4**, Fgf11, Fas, Acvr1c, Fgf9, Rps6ka2, Mapkapk3, **Fgf22**, **Pdgfb**, **Cacna2d2**, Cacna1s, **Dusp16**, **Ptprr**, **Pla2g4c**, **Rasgrp2**, **Ntf4**, **Tp53**, **Il1r2**, **Dusp10**, **Pcbp2**, **Dusp5**, **AABR07007642.1**, **Rps6ka3**, **Fgfr1**, **Pak2**, **AABR07033324.1**, **Mapt**, **Faslg**, **Hras**, Ptpn5, Mapk8ip3, **Cacna1h**, Cacna2d3, **Dusp1**, LOC108348108, **Atf4**, **Fgf5**, Mknk1, Rasgrp3, Cacna1b, Mapk13, Kras, **Cacnb3**, **Rapgef2**, **Flna**, **Ptpn7**, **LOC100912365**, **Fosl2**, Egf, Ppp3cb, **Plg**, **Hspa1b**, **Mef2c**, **Prkca**, Ikbkb, Cd14, **Pla2g4f**, Cacna2d1, **Hspa1l**, **Mapk10**, **Cacna1a**, **Mapk3**, **Gadd45g**, **Fgf7**, **Cdc25b**, Map2k3, Cacnb2, Gadd45b, **Hspb1**, **Cacng5**, Nf1, **Ngf**, **Gng12**, **Tgfb2**, **Map4k3**, Bdnf, **Fgf19**
Protein processing in endoplasmic reticulum	lncRNAs Targets	**AABR07021384.1**, **Ngly1**, **AABR07017046.1**, Pdia4, Ern1, **Ppp1r15a**, Eif2ak4, Ube2g1, **Aimp2**, Xbp1, **Sec61a2**, P4hb, Ssr1, Mbtps1, Sec24b, Pdia6, **Man1c1**, Nfe2l2, Eif2ak3, Bcap31, Skp1, Lman1l, Chek1, **Nsfl1c**, Map3k5, Ufd1, **AC135026.1**, Ube2j1, Edem3, Derl2, **Ezh2**, Map2k7, Asb3, **AABR07033324.1**, Capn1, **Ganab**, Pdia3, Hsp90aa1, AABR07028668.1, Slc35b2, Calr, Ssr3, Hyou1, Rad23a, Sel1l, **LOC689959**, Sec23a, Ube2d3, Hspa5, **Atf4**, **AABR07048012.1**, Man1a2, Dnajb12, Atf6b, **Canx**, **Dnajb1**, Lman1, Bak1, Rad23b, **Bcl2**, LOC103692716, Sec61b, Bax, **Dnaja1**, **Ube2j2**, **Capn8**, Derl1, Sec24a, **Sec63**, Mapk9, **Cryab**, Plaa, **Ero1a**, LOC103694875, Rnf5, **AABR07048013.1**, Sar1b, Atp6v1c2, Dnajc5, Syvn1, Hspa1l, Mapk10, Stub1, Svip, Dnajc5g, Dad1, Hspa2, Mbtps2, Os9, Ssr2, Erlec1, Ckap4, Ube2d2, March6, Dnajc3, Hspa1b, Rbx1, Eif2ak1, Eif2ak2, Bag1, Sel1l2, Dnajb11, Sec31a, Ubqln4, Sec23b, Hsp90ab1, Man1b1, Ell3, Ero1b
	mRANs	AABR07001519.1, **AABR07021384.1**, **Ngly1**, Mapk8, **Ezh2**, **Man1c1**, **AABR07017046.1**, **Ppp1r15a**, **Bcl2**, Fbxo2, Rrbp1, **AABR07033324.1**, Fbxo6, **Aimp2**, **Sec61a2**, **Os9**,**AABR07048012.1**, **Ganab**, **Hspa1b**, **Hspa1l**, **Ubqln2**, **Ube2j2**, **Capn8**, Hsp90b1, Hspbp1, Selenos, **Dnaja1**, **Sec63**, **LOC689959**, LOC108348108, Dnaja2, **Cryab**, Vcp, Uggt1, **Ero1a**, **Bag1**, **Atf4**, **Nsfl1c**, Ube2d1, Eif2s1, **Sar1b**, **AABR07048013.1**, **Atp6v1c2**, **Canx**, **Sec23b**, **AC135026.1**, **Hsp90ab1**, **Dnajb1**, Sec24d, **Mapk10**
AMPK signaling pathway	lncRNAs Targets	Pfkfb3, Tbc1d1, Stk11, Ppp2r5e, **Slc2a2**, **Pparg**, Irs3, Rab11b, **LOC681458**, Akt1, **Camkk2**, Ulk1, LOC100911725, Ppp2ca, Adipor1, **G6pc**, Ccna1, Rps6kb2, **Creb3l2**, Msl2, Pik3r2, Gys1, Cpt1c, Ppp2r1b, **Cab39l**, **Scd2**, G6pc3, Prkag2, Elavl1, AABR07044925.1, Fbp2, LOC100910771, Ppp2r2d, Pik3cd, Ppp2r3b, **Fasn**, Pck1, Srebf1, Pik3ca, AC121639.1, Pfkfb4, **Scd4**, Lipe, **Foxo1**, Cbarp, Ppp2r1a, **Angptl7**, Pdpk1, Akt2, Rptor, Pck2, **Slc2a4**, Igf1r, Ppp2r5c, Hmgcr, Ccdc103, Gpha2, Prkab2, Rab10, Tmem206, **Mtor**, **Creb5**, **Fbp1**, Akt1s1, **Ubxn8**, Foxo3, **Acacb**, Hnf4a, Ccnd1, Ppp2r5b, Creb1, Mlycd, **Prkag3**, Irs2, Pik3r3, Akt3, **Ppp2r5a**, Ins2, Rab2a, Prkab1, **Lep**, Rab14, Pfkfb1, **Pik3r1**

	mRANs	**Slc2a2**, Creb3l4, Eef2, **Foxo1**, **LOC681458**, Creb3l1, **G6pc**, LOC100910021, **Cab39l**, Gys2, **Creb3l2**, **Scd2**, **Fbp1**, Adra1a, Melk, **Pparg**, **Fasn**, Acaca, Pfkm, Ppp2r2b, **Scd4**, Scd, **Angptl7**, Ccna2, **Slc2a4**, Pik3r5, Ppargc1a, **Mtor**, **Creb5**, **Ubxn8**, Lepr, **Acacb**, **Camkk2**, **Prkag3**, **Ppp2r5a**, Insr, **Lep**, **Pik3r1**
cGMP-PKG signaling pathway	lncRNAs Targets	Gna12, **Atp2b3**, Rad9a, **Atp1b3**, **Plcb3**, **Kcnmb3**, LOC100911796, Ppp1r12a, Gucy1a2, **Slc8a3**, Itpr3, Adcy5, Myl12a, **Comtd1**, Atp2b1, **LOC100912262**, **Adcy7**, Nfatc1, Adcy9, Irs2, Nfatc2, Mef2d, Adrb3, Ppp3cc, **Atp1a1**, Rhoa, Akt3, **Adcy1**, **Pik3r1**, Vdac2, Irs3, Akt1, **Adrb2**, **Atp1a4**, Kcnmb4, **Creb3l2**, **AC106648.1**, **Pln**, **Adcy6**, **Atp2b4**, Pde3b, Adcy4, AABR07005775.1, Gnai3, **Itpr1**, Vdac3, **Atf4**, **Creb5**, Rock2, Atf6b, **Plcb1**, Pik3r3, **Npr2**, Gtf2ird1, Gtf2i, Adra2b, Ppif, **Mylk2**, Raf1, Atp1b2, Calm1, Adrb1, **Atp4a**, **Ednra**, Ppp3r1, Gna13, Akt2, **Mef2c**, Vdac1, Slc25a31, Plcb2, Ppp1cc, AABR07027466.1, **Atp1a2**, Mef2a, Pik3ca, Slc25a4, Ppp1ca, **Prkg2**, **Oprd1**, **Myl9**, Pik3r2, Itpr2, **Mapk3**, **Tcta**, Pik3cd, **Kcnma1**, Creb1, Uqcc2, **Kcnu1**, **Adora3**, AABR07061707.1, NEWGENE_1307313, **AABR07062512.1**, Nfatc4, Vasp, **Plcb4**, Cacna1d, Map2k1, Bad, **Nppb**, AABR07062799.2, **Mef2b**, AC136025.1, Adra2a, Ins2
	mRANs	Cacna1s, Creb3l4, Fxyd2, Gnaq, Atp1a3, **Prkg2**, Pde3a, Slc8a1, **Atp1b3**, Atp1b4, **Oprd1**, **Myl9**, **Plcb3**, **Comtd1**, **Mapk3**, **Creb3l2**, **Kcnmb3**, **AC106648.1**, **Mylk2**, Gucy1b2, **Atp1a4**, Itpr3, **Adrb2**, Adra1a, Mylk, Adcy2, **Atf4**, **Kcnma1**, Creb3l1, **Atp4a**, **Kcnu1**, **Mef2c**, **Atp2b4**, **Ednra**, **Adora3**, Mylk3, **LOC100912262**, **Adcy7**, **AABR07062512.1**, Ppp3cb, Pde2a, Pik3r5, Bdkrb2, Cacna1c, **Atp2b3**, Insr, **Itpr1**, **Tcta**, Gnaz, **Adcy6**, **Creb5**, **Slc8a3**, Npr1, Atp2a3, **Plcb4**, **Atp1a2**, **Atp1a1**, Mrvi1, LOC100910021, Adra1b, **Plcb1**, Rgs2, **Nppb**, **Mef2b**, **Pln**, **Npr2**, Cngb1, Ednrb, **Adcy1**, **Pik3r1**
TGF-beta signaling pathway	lncRNAs Targets	**Nodal**, Smad1, Gdf7, Smurf2, Zfyve9, **Ezh2**, **Tfdp1**, **Smad9**, **Ltbp1**, **Smad6**, Ppp2ca, AABR07058539.1, **Rbl1**, Rps6kb2, **Mapk3**, Acvr2a, Smad2, **Tcta**, **Sp1**, Smad4, **Id3**, Smad5, E2f4, **Bmp6**, Bmpr1a, Crebbp, Acvr1b, Tgfbr2, Ppp2r1a, Smurf1, Tnf, Rbx1, Myc, **Amhr2**, **Tgfb2**, Smad7, Orc4, Skp1, E2f5, **Inhba**, Smad3, LOC103694380, **Ubxn8**, **Lefty1**, Rhoa, **Bmp7**, **Bmpr2**, Tgfbr1, Chrd, Ppp2r1b, Lefty2, **Bmp8a**, Id1
	mRANs	**Rbl1**, Id2, **Ezh2**, **Tfdp1**, **Smad9**, **Bmp8a**, Gdf5, **Mapk3**, **Bmp6**, **Inhba**, **Sp1**, **Id3**, Acvr1c, Id4, **Nodal**, **Tgfb2**, **Amhr2**, Bambi, **Tcta**, Bmpr1b, **Ubxn8**, LOC103691556, **Bmp7**, **Bmpr2**, **Lefty1**, **Smad6**, **Ltbp1**, Acvr1
Ras signaling pathway	lncRNAs Targets	**Efna5**, **Fgf18**, **Bcl2l1**, Rel, **Rasa4**, **Pla2g4c**, Gnb5, AABR07003173.1, Pak4, Sos2, Pla2g2a, Fgf2, **Shc3**, Shc1, Grb2, Htr7, **Fgf22**, Gng5, **Rab5b**, **Pdgfb**, Pld2, **Shc4**, Pla2g3, Efna3, Pla1a, Fgf17, AABR07043601.3, **Plce1**, Rhoa, Fgfr3, **Rasgrp2**, Akt3, Fgf1, **Pik3r1**, Foxo4, Akt1, **AABR07007642.1**, **AC098008.1**, Vegfa, LOC108348044, **Fgfr1**, **Pak2**, **Faslg**, Map2k1, **Hras**, **Rasa3**, Pak6, **Arf6**, Gnb3, Prkaca, Rasa2, Ngfr, **Angpt2**, Flt4, Rela, Chuk, Cdc42, Sos1, Rap1a, Gnb2, **Plcg1**, Pla2g6, AABR07051241.1, **Fgf5**, Gng13, Pik3r3, Fgf21, Rac2, **Rgl1**, **Pla2g1b**, **Syngap1**, Gng10, Gng3, Pla2g4d, Fgf6, Stk4, **Gngt2**, Fgf16, Rasgrf1, Prkacb, Shc2, LOC100912034, Raf1, Calm1, Pla2g12a, **Pla2g4f**, Rapgef5, Akt2, Fgf23, Grin1, Mapk9, Rap1b, **Pak3**, **Prkca**, Efna4, Fgfr4, Pla2g10, **Rassf1**, **Gab2**, **Gng2**, Pik3ca, **Zap70**, **Mapk10**, Rasgrp1, **Rasal3**, Igf1r, **Exoc2**, **Grin2a**, **Flt1**, Pla2g16, Pik3r2, **Mapk3**, **Fgf7**, **Epha2**, **Tcta**, LOC108348190, LOC100910732, LOC102552659, Pik3cd, **Pld1**, Ralbp1, **Efna1**, Fgf3, **Ets1**, Ras, Fgf8, Gng14, **Ngf**, **Gng12**, Rasal1, Bad, Csf1, **Csf1r**, Rgl2, Pla2g5, **Gab1**, Fgf4, Ins2, AABR07033987.1, **Fgf19**
	mRANs	**Efna5**, Abl1, Efna2, Kras, **Rasal3**, **Arf6**, **Gab1**, **Syngap1**, Fgfr2, **Shc4**, **Rasa4**, **AABR07007642.1**, Vegfb, **AC098008.1**, **Exoc2**, **Grin2a**, **Fgfr1**, **Pak2**, **Mapk3**, Fgf11, **Faslg**, Plcg2, **Fgf7**, **Epha2**, Rasgrp3, **Rgl1**, **Tcta**, **Plcg1**, **Hras**, Ksr1, Kit, **Pld1**, **Csf1r**, **Rasa3**, Mapk8, **Shc3**, **Gngt2**, **Rassf1**, Egf, Abl2, Kdr, **Ets1**, Afdn, **Fgf22**, Rasgrp4, Ksr2, Nf1, **Angpt2**, **Ngf**, **Gng12**, Pla2g12b, **Rab5b**, Ets2, Pik3r5, Grin2b, **Pak3**, **Pla2g1b**, Uxt, Ralgds, Brap, **Flt1**, **Fgf18**, Fgf9, Ikbkb, **Prkca**, **Pdgfb**, **Fgf5**, Lat, **Plce1**, **Fgf19**, **Bcl2l1**, **Gab2**, **Rasgrp2**, **Pla2g4f**, **Gng2**, **Pla2g4c**, LOC100910021, **Efna1**, Insr, Pak7, **Zap70**, **Mapk10**, **Pik3r1**
ErbB signaling pathway	lncRNAs Targets	Braf, **Cdkn1a**, Pak4, **Prkca**, **Shc4**, Akt1, Map2k7, AABR07003173.1, Nck1, **Pak2**, Rps6kb2, Pik3r2, Stat5a, Sos2, Map2k1, **Plcg1**, **Hras**, LOC108348190, **Angptl7**, Raf1, LOC100910732, LOC102552659, Pik3cd, Camk2d, **Shc3**, Pak6, Pik3ca, Shc1, **Cdkn1b**, **Camk2a**, Grb2, Akt2, Nck2, Myc, Mapk9, Nrg2, Bad, Cbl, Crk, Sos1, **Mtor**, **Erbb3**, AABR07043601.3, Jun, Stat5b, **Nrg1**, **Gab1**, **Mapk3**, Pik3r3, Akt3, Shc2, **Cblb**, **Pik3r1**, Ptk2, **Mapk10**, **Pak3**
	mRANs	Abl1, **Cdkn1a**, Kras, Mapk8, Uxt, Cblc, **Shc4**, Gsk3b, Erbb2, LOC100910021, **Pak2**, **Mapk3**, Plcg2, **Plcg1**, **Hras**, Ereg, Areg, Egf, Abl2,**Cdkn1b**, **Camk2a**, **Shc3**, **Angptl7**, Pik3r5, **Pak3**, **Prkca**, **Mtor**, **Erbb3**, **Nrg1**, **Gab1**, **Cblb**, Pak7, **Mapk10**, **Pik3r1**
FoxO signaling pathway	lncRNAs Targets	**Agap2**, Braf, **Cdkn1a**, Gabarapl1, Stk11, **Slc2a2**, Crebbp, Foxo4, Irs3, AABR07003173.1, Akt1, **Bnip3**, Prmt1, Skp2, AABR07058539.1, **G6pc**, Pik3r2, **Mapk3**, Stk4, **Gadd45g**, **Ccnd2**, LOC102552659, Map2k1, G6pc3, Prkag2, Stat3, Smad4, LOC108348190, AABR07044925.1, Sos2, Raf1, Gabarap, Pik3cd, Mapk11, **Faslg**, Pck1, Gadd45a, Pik3ca, **Foxo6**, **Plk4**, Atg12, Gabarapl2, **Cdkn1b**, **Foxo1**, Cbarp, Tgfbr2, Grb2, Pdpk1, Akt2, Pck2, S1pr4, **Slc2a4**, **Tgfb2**, Pten, Chuk, Igf1r, Irs2, Sgk3, Mapk14, Prkab2, Sos1, Mapk9, Smad3, **Ccnb1**, Mapk12, **Mdm2**, Smad2, Foxo3, Cdk2, Ccnd1, **Hras**, **Homer1**, **Sgk1**, **Setd7**, **Prkag3**, Pik3r3, Akt3, Ins2, Prkab1, **Grm1**, **Mapk10**, **Pik3r1**

	mRANs	**Agap2**, **Sgk1**, **Cdkn1a**, Plk1, Kras, **Slc2a2**, Mapk8, **Foxo1**, Fbxo25, Acvr1c, **G6pc**, Ccnb3, **Mapk3**, Rag2, **Faslg**, **Gadd45g**, **Ccnd2**, Homer2, **Hras**, Melk, Gadd45b, Ccng2, **Foxo6**, Egf, **Cdkn1b**, Il6, **Tgfb2**, **Slc2a4**, Pik3r5, Sod2, **Plk4**, Plk3, Rag1, Ikbkb, **Mdm2**, **Ccnb1**, LOC100910021, **Homer1**, **Setd7**, **Prkag3**, **Bnip3**, Insr, Mapk13, **Grm1**, **Mapk10**, **Pik3r1**
Jak-STAT signaling pathway	lncRNAs Targets	Spred1, **Bcl2l1**, Stam2, Stat1, AABR07003173.1, Pias1, Crlf2, **Sos2**, Il6st, Socs1, Ifnl3, Crebbp, Grb2, **Socs2**, Cbl, Il13, Il20, **Il12rb1**, Ifngr2, Akt3, **Cblb**, **Pik3r1**, Tpo, Akt1, Epo, AC098008.1, Il5ra, **Ccnd2**, Prlr, Tyk2, **Il20rb**, Il2ra, Il5, Il21, **Olr741**, **Epor**, **Ctf1**, Il10rb, **Clcf1**, Sos1, Ifna4, **Socs7**, Ccnd1, Ifnl1, Spry2, Pik3r3, Serbp1, **Lep**, **Pim1**, **Mpl**, **Il24**, Irf9, Stat3, Akt2, Il2, Ccnd3, **Il2rg**, **Socs3**, Gh1, Il9, Ifnar1, **Il2rb**, Stat5b, Ifnb1, Csf2ra, Pik3ca, **Il12rb2**, Socs5, AABR07058539.1, Pik3r2, Ifnar2, Il6r, Stat5a, **Il19**, Ifna11, Pik3cd, Il3, Ghr, Il15, Myc, **Ptpn6**, Csf2rb, **Cntfr**, Il11ra1, Ifnlr1
	mRANs	**Il12rb2**, Il15ra, **Bcl2l1**, Il22, Il23r, **Pim1**, **Mpl**, Cblc, **Il24**, AC098008.1, LOC100910021, Spred3, Ifne, **Ccnd2**, **Il19**, **Socs1**, **Il20rb**, Tslp, **Olr741**, Lifr, Osmr, **Epor**, **Ctf1**, **Il2rb**, Il6, **Socs2**, **Clcf1**, Il10ra, Il12a, **Cntfr**, **Il2rg**, **Socs3**, **Socs7**, **Cblb**, **Il12rb1**, Pias3, Csf3r, Lepr, Pik3r5, Il22ra1, Il11, **Ptpn6**, Il4r, **Lep**, Stam, **Pik3r1**
PI3K-Akt signaling pathway	lncRNAs Targets	**Efna5**, **Fgf18**, Stk11, **Bcl2l1**, Ywhag, Eif4e2, **Tnn**, **Tp53**, Gnb5, AABR07003173.1, Mlst8, Sos2, **Lama5**, Efna4, Cd19, Ywhae, **Them4**, Ppp2r2d, Fgf2, Lamc3, **C1qtnf1**, Col27a1, **Cdkn1b**, **Fn1**, Ptger1, Grb2, Pdpk1, Pck2, Gng5, Pkn1, **Pdgfb**, Ppp2r5e, Tmem206, **Mtor**, Fgf17, **Mdm2**, Foxo3, Flt4, **Lama4**, Fgfr3, **Efna1**, Akt3, Comp, Itgb1, **Lamc2**, **Pik3r1**, **Itga11**, Akt1, Epo, **AC098008.1**, Vegfa, Ppp2ca, **G6pc**, **Col4a1**, **Flt1**, **Itgb6**, **Faslg**, **Ccnd2**, Map2k1, **Hras**, Bricd5, Ppp2r3b, Prlr, **Col1a1**, Il2ra, Slc35b2, Rptor, Gnb3, **Epor**, Cbarp, Ywhah, Ngfr, **Angpt2**, Tspan31, **AABR07073181.1**, Rela, Pten, Chuk, Ppp2r5b, Sgk3, Gpha2, Sos1, Itga4, **Atf4**, **Creb5**, G6pc3, Pkn2, Ifna4, **Fgf5**, Ccnd1, Atf6b, **Mapk3**, Gng13, Pik3r3, **Ppp2r5a**, Eif4e, Fgf21, **Cdkn1a**, Cthrc1, Gng10, Gng3, **Ddit4**, Cdk4, Casp9, **Bcl2**, LOC103692716, **Creb3l2**, Msl2, Fgf6, **Gngt2**, Fgf16, Ppp2r5c, Rxra, **Col5a1**, LOC100912034, Raf1, Lpar5, Cdc37, Tnr, Gnb2, Gh1, Itga3, Ppp2r1a, Pck1, Il2, Fgf23, Ccnd3, Cdk2, **Prkca**, Col4a6, Thbs2, Ifnar1, **Il2rb**, **Tlr2**, Creb1, Ifnb1, Ppp2r1b, **Gng2**, Pik3ca, **Tnc**, Nr4a1, Ptk2, **Spp1**, **Sgk1**, **Fgf22**, **Brca1**, Igf1r, **Itga9**, **Reln**, Efna3, Rps6kb2, Ifnar2, Il6r, Pik3r2, Gys1, **Fgf7**, **Epha2**, **Itga10**, Ifna11, LOC108348190, **Angptl7**, Pik3ap1, Fgf1, LOC102552659, Pik3cd, Akt2, **Col5a3**, **Fgfr1**, **Cela2a**, Il3, Fgf3, **Thbs3**, Ghr, Lpar1, Fgf8, Gng14, **Ngf**, **Gng12**, **Lamc1**, Myc, Bad, Csf1, **Itgb8**, **Csf1r**, **Itgb4**, **Ubxn8**, Fgfr4, **Col4a2**, Cdk6, **Il2rg**, **Hsp90ab1**, Fgf4, Ins2, Ibsp, AABR07033987.1, **Fgf19**, Hsp90aa1
	mRANs	**Efna5**, **Fgf18**, **Bcl2l1**, **Tnn**, Fgfr2, Vegfb, **Tp53**, Lamb3, Fgf11, **Lama5**, Itga2, **Them4**, Col2a1, Kdr, Hsp90b1, **C1qtnf1**, Lpar6, Ikbkb, **Cdkn1b**, **Fn1**, **Angptl7**, **Angpt2**, Il6,**Fgf22**, Itga1, **Col4a2**, **Mtor**, Fgf9, **Mdm2**, **Lama4**, **Lamc2**, **Pik3r1**, Efna2, **Itga11**, Col5a2, **AC098008.1**, **G6pc**, **Col4a1**, **Flt1**, **Itgb6**, **Faslg**, F2r, **Ccnd2**, Vwf, **Hras**, Ccne1, Colec10, Melk, Itgb3, Ccne2, Ppp2r2b, **Itgb4**, **Epor**, Col6a1, **AABR07073181.1**, **Cela2a**, Col6a5, **Atf4**, **Creb5**, Itga8, AABR07030375.3, Csf3r, **Fgf5**, **Col5a3**, **Ppp2r5a**, Kit, Thbs4, Cdkn1a, Kras, Lama2, **Ddit4**, **Bcl2**, LOC100910021, Col11a1, **Creb3l2**, **Col1a1**, **Gngt2**, AABR07031193.1, **Col5a1**, Col3a1, Itga7, Creb3l1, Egf, Itgav, Pik3r5, **Prkca**, **Itga10**, Adipoq, **Il2rb**, **Tlr2**, **Gng2**, **Tnc**, Insr, Il4r, AABR07068042.1, **Spp1**, **Sgk1**, Itga6, Creb3l4, Col1a2, Col4a5, Lamb1, **Itga9**, Gsk3b, **Reln**, **Mapk3**, **Fgf7**, **Epha2**, Lamb2, AABR07030544.1, **Brca1**, **Fgfr1**, **Efna1**, **Thbs3**, Osmr, Gys2, **Ngf**, **Gng12**, **Lamc1**, Myb, **Itgb8**, **Csf1r**, **Ubxn8**, Chad, **Pdgfb**, **Il2rg**, **Hsp90ab1**, **Fgf19**
cAMP signaling pathway	lncRNAs Targets	Braf, Grin3b, Sstr5, Rad9a, **Atp1b3**, Ppara, Ppp1r12a, Adcy5, **Pde4a**, Myl12a, Camk2d, Ppp1cc, Arap3, Atp2b1, Crebbp, Rapgef3, **Adcy7**, Ras, Adcy9, Orai1, Pld2, **Atp2b3**, Htr6, **Adrb2**, **Adcy6**, Htr4, Jun, **Plce1**, **Atp1a1**, Rhoa, Akt3, Adcy1, Grin3a, **Pik3r1**, Pde4c, Akt1, **Grin2a**, **Atp1a4**, Fshb, Map2k1, **Pln**, AC121639.1, **Atp2b4**, Prkaca, Vav2, **Tshr**, Pde3b, Rela, Gnai3, Ffar2, **Gria2**, Rap1a, Atp1b2, **Creb5**, AABR07051241.1, Rock2, Abcc4, Acox1, **Vipr2**, Pik3r3, **Gli3**, **Hcn2**, Rac2, **Fshr**, **Creb3l2**, Oxtr, Prkacb, Raf1, Drd2, Calm1, Adrb1, **Atp4a**, **Fosl2**, **Ednra**, **Cnga1**, **Grin2c**, Creb1, Grin1, Mapk9, Rap1b, Hcar2, **Pde4b**, Htr1d, Htr1f, Nfatc1, **Atp1a2**, Pik3ca, **Mapk10**, AABR07058539.1, Lipe, Ppp1ca, Rapgef4, Fxyd1, **Myl9**, Hcar1, Pik3r2, **Mapk3**, **Tcta**, Pik3cd, **Pld1**, Adcy4, Fos, Akt2, **Adcy10**, **Camk2a**, **Grin2d**, Cacna1d, Bad, Gnas, Vav1, Gabbr1, **Sox9**
	mRANs	**Hcn2**, Cacna1s, Gria1, Ptch1, **Fshr**, Fxyd2, Mapk8, Ghrl, Atp1a3, Slc9a1, Camk4, **Adrb2**, **Atp1b3**, Atp1b4, Sstr2, **Myl9**, Gpr119, Gipr, **Grin2a**, **Mapk3**, **Atp1a4**, Tnni3, F2r, Pde3a, **Creb3l2**, **Tcta**, **Pde4b**, **Pde4a**, Gnaz, Creb3l4, Adcyap1r1, **Pld1**, **Sox9**, Creb3l1, **Adcy10**, Gria3, **Atp4a**, **Pik3r1**, **Fosl2**, **Atp2b4**, Ryr2, **Ednra**, **Cnga1**, **Grin2c**, **Adcy7**,**Grin2d**, **Tshr**, Fxyd1, Pik3r5, Grin2b, Cacna1c, Gli1, Adcy2, **Gria2**, **Atp2b3**, **Adcy6**, **Creb5**, **Camk2a**, Afdn, Npr1, LOC100912228, Atp2a3, Nfkbia, Npy, Cngb1, **Atp1a2**, **Atp1a1**, Cnga4, LOC100910021, Bdnf, Cnga3, **Plce1**, **Vipr2**, **Pln**, Adcy1, Gria4, **Gli3**, **Mapk10**, Ptger3
mTOR signaling pathway	lncRNAs Targets	Braf, Stk11, Eif4e2, Akt1, **Ddit4**, Ulk1, Vegfa, Akt1s1, Rragd, **Rps6ka3**, Rps6kb2, **Cab39l**, Mlst8, Pik3r2, LOC108348096, Pik3cd, Hif1a, Pik3r3, Tnf, Cbarp, **Angptl7**, Pdpk1, Akt2, Rptor, Ins2, Pten, Ulk2, **Prkca**, **Mtor**, Ulk3, LOC103694380, Bricd5, RragB, **Mapk3**, Pik3ca, Akt3, Eif4e, Rps6ka1, **Pik3r1**
	mRANs	Ikbkb, **Mtor**, Pik3r5, **Prkca**, Melk, **Ddit4**, Rps6ka2, **Rps6ka3**, **Angptl7**, LOC100910021, **Mapk3**, **Cab39l**, **Pik3r1**
TNF signaling pathway	lncRNAs Targets	Map2k4, **Map3k8**, Traf5, Atf6b, Map3k5, Rps6ka4, **Traf1**, Akt1, **Birc3**, Csf1, Map2k7, Casp8, Pik3r2, **Creb3l2**, **Mapk3**, Tnfrsf1a, Ccl12, Map2k1, Map3k14, **Tradd**, **Cebpb**, LOC100910771, Itch, Mlkl, Pik3cd, Mapk11, **Mmp9**, Fos, Akt2, **Icam1**,

		Pik3ca, **Fosl2**, Tab3, Ripk1, Ripk3, **Mmp14**, Il15, Tnf, Junb, Tnfrsf1b, Mapk9, Birc2, Casp3, **Socs3**, Rela, **Atf4**, **Creb5**, Mapk12, Jun, **Ccl2**, Lta, Fadd, Chuk, Tab1, Traf3, Creb1, Casp7, Pik3r3, Akt3, LOC103694380, Mapk14, Cflar, **Mapk10**, **Pik3r1**
	mRANs	**Map3k8**, Creb3l4, Mapk8, **Traf1**, Mmp15, LOC100910021, **Mapk3**, **Creb3l2**, Pgam5, Fas, Map2k3, **Tradd**, **Cebpb**, Edn1, **Mmp9**, Creb3l1, **Icam1**, **Birc3**, Ifi47, **Mmp14**, Cxcl1, Il6, Cx3cl1, Pik3r5, **Socs3**, **Atf4**, **Creb5**, Huwe1, Ikbkb, Il18r1, Nfkbia, **Ccl2**, Vcam1, **Fosl2**, Cxcl3, Ccl5, Bcl3, Ccl20, Mmp3, Mapk13, **Mapk10**, **Pik3r1**
Wnt signaling pathway	lncRNAs Targets	Psen1, Daam1, Mmp7, Lzic, Nfatc1, **Ezh2**, Wif1, Fzd6, **Fosl1**, LOC100910771, **Tcf7**, Plcb2, **Camk2a**, **Wnt10a**, AABR07058539.1, **Plcb3**, **Plcb1**, Ctnnbip1, Prkaca, **Ccnd2**, **Lef1**, **Tcta**, Smad4, Smad3, Wnt7b, Nfatc4, Camk2d, Wnt5a, Ppp3cc, Wnt3a, Fbxw11, **Daam2**, **Tcf7l2**, Csnk1a1, **Wnt7a**, Dkk1, Wnt2b, Ppp3r1, Crebbp, **Ctbp2**, **Tp53**, Vangl1, Dvl1, LOC100909849, Wnt9a, Prickle2, Rbx1, Sfrp5, Myc, Mapk9, Ccnd3, **Plcb4**, **Dvl3**, Skp1, Nfatc2, **Prkca**, **Wnt4**, **Fzd1**, **Sfrp2**, Rock2, **Prickle1**, Dvl2, **Tbl1xr1**, Jun, Ccnd1, Rhoa, Rac2, Fzd8, Csnk2b, Prkacb, **Fzd5**, **Apc2**, Siah1, Cacybp, **Wnt6**, Tcf7l1, Smad2, **Mapk10**, Axin2
	mRANs	**Fosl1**, Fzd9, Mapk8, **Ezh2**, **Fzd1**, **Tcf7**, Gsk3b, **Camk2a**, **Wnt10a**, **Plcb3**, **Lef1**, Sfrp4, **Ccnd2**, **Tcta**, **Wnt4**, Wnt11, **Tcf7l2**, **Wnt7a**, Fzd4, Sfrp1, **Ctbp2**, **Tp53**, Gpc4, Ppp3cb, **Plcb4**, Bambi, **Dvl3**, **Prkca**, Vangl2, **Sfrp2**, **Prickle1**, **Tbl1xr1**, Porcn, AABR07007000.1, **Plcb1**, Tbl1x, **Fzd5**, **Apc2**, **Daam2**, Apc, Cacybp, **Wnt6**, **Mapk10**
NF-kappa B signaling pathway	lncRNAs Targets	Irak1, Traf5, **Bcl2l1**, Traf3, **Traf1**, LOC103689974, Tnfrsf13c, Tirap, **Bcl2**, Relb, Ltbr, Lyn, Tnfrsf1a, Ube2i, **Plcg1**, Map3k14, **Tradd**, Ltb, Erc1, LOC100910771, Nfkb2, Ccl19, **Ddx58**, **Icam1**, **Ticam2**, **Birc3**, Tab3, Ripk1, AABR07026596.2, LOC102553386, Tnf, Rela, Irak4, Erc2, LOC103694380, LOC103694381, Plau, Birc2, Chuk, Tab1, Cxcl12, Csnk2b, Il1r1, Lta, **AC098008.1**, Bcl10, Tnfsf14, **Zap70**, Cflar, **Tnfrsf11a**, **Tnfsf13b**
	mRANs	Plcg2, **Bcl2l1**, **Ddx58**, Hck, **Traf1**, **AC098008.1**, **Bcl2**, Myd88, **Plcg1**, **Tradd**, Gadd45b, Cd40, **Icam1**, Bcl2a1, **Ticam2**, **Birc3**, Ikbkb, Nfkbia, Lat, Vcam1, Cd14, Plat, **Zap70**, **Tnfrsf11a**, **Tnfsf13b**
Rap1 signaling pathway	lncRNAs Targets	**Efna5**, **Fgf18**, **Fpr1**, **Cdh1**, **Plcb3**, Skap1, Adcy5, Fgf2, Mapk11, Arap3, Rapgef3, **Adcy7**, **Angpt2**, **Fgf22**, Itgal, Actg1, **Pdgfb**, Adcy9, Rapgef6, **Ctnnd1**, Efna3, Fgf17, **Plce1**, Rhoa, **Prkd3**, Prkcz, Akt3, Itgb1, Mapk14, **Adcy1**, **Pik3r1**, Igf1r, Lpar5, Fgfr3, Akt1, **Farp2**, Vegfa, **Rasgrp2**, **Fgfr1**, **Grin2a**, Map2k1, **Hras**, **Adcy6**, Fgf16, Flt4, Gnai3, Cdc42, Fgf6, Rap1a, **Cnr1**, AABR07051241.1, **Fgf5**, Crk, **Mapk3**, **Plcb1**, Pik3r3, Fgf21, **Sipa1**, Braf, Rac2, Magi3, **Rapgef2**, Ngfr, **Plcg1**, **Tln1**, Raf1, Drd2, Calm1, **Pfn4**, Rapgef5, Akt2, Bcar1, Fgf23, Grin1, Rap1b, **Prkca**, **Gnao1**, Efna4, Plcb2, **Pard6a**, Pik3ca, Id1, Map2k4, Rapgef4, Mk1, Lpar1, Actb, **Sipa1l1**, **Flt1**, Pik3r2, **Magi1**, **Tln2**, **Epha2**, **Tcta**, LOC108348190, Fgf1, LOC102552659, Pik3cd, **Efna1**, Fgf3, **Fgf7**, Rras, Fgf8, **Ngf**, **Adora2b**, Vasp, **Plcb4**, Csf1, **Csf1r**, Mapk12, Gnas, Fgfr4, Adcy4, Fgf4, Ins2, **Fgf19**
	mRANs	**Grin2a**, **Efna5**, Efna2, Sipa1l2, Kras, **Fpr1**, Map2k3, Gnaq, Fgfr2, **Adora2b**, Vegfb, **Farp2**, LOC100910021, **Plcb3**, **Fgfr1**, **Sipa1l1**, **Mapk3**, Fgf11, **Magi1**, F2r, **Tln2**,**Epha2**, Rasgrp3, **Fgf7**, **Tcta**, Dock4, **Hras**, **Tln1**, Kit, **Ctnnd1**, Adcy2, AABR07030544.1, Itgb3, **Pfn4**, **Csf1r**, **Pdgfb**, **Adcy6**, Egf, Kdr, Afdn, **Plcb4**, **Fgf22**, **Adcy7**, **Angpt2**, **Ngf**, Pard6g, **Rapgef2**, **Cdh1**, Pik3r5, Lcp2, **Flt1**, **Sipa1**, Pard6b, **Prkca**, **Gnao1**, Ralgds, Gnaz, **Fgf18**, Fgf9, **Plcg1**, P2ry1, Rap1gap, **Fgf5**, Lat, **Plce1**, **Prkd3**, **Rasgrp2**, **Plcb1**, **Pard6a**, Grin2b, **Cnr1**, **Efna1**, **Adcy1**, Mapk13, **Fgf19**, Insr, **Pik3r1**
p53 signaling pathway	lncRNAs Targets	Casp8, **Cdkn1a**, Sesn1, Igfbp3, **Tp53**, Serpine1, Cdk4, Casp9, Pten, Bax, Chek2, **Gadd45g**, **Ccnd2**, Tp73, Zmat3, **Sesn3**, Mdm4, **Ddb2**, **Cela2a**, Serpinb5, **Rrm2**, Cd82, Tspan31, Sfn, Ccnd3, Cdk2, Cop1, Casp3, Gadd45a, **Rrm2b**, **Ccnb1**, **Mdm2**, **LOC100359539**, Atr, **Cdk1**, Cdk6, Ccnd1, Siah1, AABR07009965.1
	mRANs	**Cdkn1a**, Rchy1, **Tp53**, Ccnb3, **Gadd45g**, **Ccnd2**, Fas, Ccne1, **Sesn3**, Gadd45b, Ccng2, Ccne2, **Rrm2**, **Ddb2**, Sesn2, **Cela2a**, Pmaip1, LOC100363502, **Rrm2b**, **Mdm2**, **LOC100359539**, Steap3, **Ccnb1**, **Cdk1**
Calcium signaling pathway	lncRNAs Targets	**Plcb3**, Chrm3, Htr5a, **Itpr3**, Adrb3, **Comtd1**, Chrna7, Camk2d, Atp2b1, **Adcy7**, Htr7, Orai2, **Nos1**, **Atp2b3**, AABR07005775.1, Htr6, **Adrb2**, Htr4, Ppp3cc, Ltb4r2, **Plce1**, **Phkg1**, Stim1, Adcy1, Vdac2, **Camk2a**, **P2rx4**, **Grin2a**, P2rx5, Tnnc2, **Cacna1h**, **Atp2b4**, **Plcd4**, Prkaca, Hrh1, **Itpr1**, Vdac3, **Slc8a3**, Htr2a, AABR07051241.1, **Plcb1**, Prkacb, LOC100909648, Pde1c, **Tacr2**, Phkb, Ppif, Oxtr, **Mylk2**, **Plcg1**, **Gnas**, Calm1, Adrb1, **Ednra**, Ppp3r1, **Grin2c**, Gna15, Orai3, Grin1, Tbxa2r, **Prkca**, Vdac1, Slc25a31, Plcb2, **Erbb3**, AABR07027466.1, **Pln**, Cacna1g, Slc25a4, **Cacna1a**, Tacr1, P2rx7, LOC102552659, Adcy4, Uqcc2, **Avpr1b**, AABR07061707.1, **AABR07062512.1**, **Grin2d**, Chrm5, **Adora2b**, Sphk1, **Plcb4**, Cacna1d, **Gnas**, Itpr2, Orai1, Ntsr1, **Grm1**
	mRANs	Cacna1s, **Cacna1a**, AABR07037995.1, Ryr1, Htr5b, Gnaq, **Tacr2**, Gna14, Cacna1c, Camk4, Slc8a1, Mlnr, **Adora2b**, **Camk2a**, Ednrb, Ptger3, Grpr, **P2rx4**, **Plcb3**, **Plcb1**, F2r, **Mylk2**, **Plcg1**, **Itpr3**, **Gnas**, **Adrb2**, Adra1a, **AABR07062512.1**, P2rx6, Adcy2, **Comtd1**, Ppp3cb, **Cacna1h**, **Phkg1**, **Itpr1**, **Avpr1b**, Ryr2, **Ednra**, Ptk2b, **Grin2c**, **Adcy7**, P2rx2, **Grin2d**, Ryr3, **Plcd4**, Phka1, Gnal,

		Plcb4, Bdkrb2, Plcg2, Erbb2, Atp2b3, Prkca, Grin2a, Atp2a3, Itpkb, Slc8a3, Dlec1, Itpka, Mylk3, Erbb3, P2rx1, Cacna1b, Plce1, Adra1b, Atp2b4, Mylk, Nos1, Pln, Adcy1, Grm1, Rpl18

mRNA–lncRNA–miRNA interaction network analysis

Co-expression is confirmed to be able to predict and evaluate the function of lncRNAs, thus mRNA–lncRNA–miRNA co-expression network with statistically DE mRNA, lncRNA and miRNA was built (Figure 6A). Figure 6B showed 161 up-regulated lncRNAs, 23 up-regulated mRNAs and 11 down-regulated miRNAs were included in this interaction network. Figure 6C showed 180 down-regulated lncRNAs, 79 down-regulated mRNAs and 13 up-regulated miRNAs were included in this interaction network. Among this network, several up-regulated or down-regulated lncRNAs were at the key junction points of the regulatory network, which can be used as important targets for further research, such as TCONS_00142807, TCONS_00050289, TCONS_00008543, ENSRNOT00000081689 and TCONS_00089281. Several differentially expressed mRNA at network nodes can also be used as key targets for research, such as ENSRNOT00000071420 (Tk1), ENSRNOT00000002119 (RGD1563888), ENSRNOT00000066211 (Tmem243), ENSRNOT00000026392 (Adprhl1), ENSRNOT00000010619 (Timm10), etc.

Protein-Protein interaction network

The target genes of DE lncRNAs related KEGG apoptosis pathway was mapped into PPI. Figure 7A showed the combined bioinformatics analysis of DE mRNA genes and target genes of lncRNAs. Figure 7B showed the PPI between confluent proteins. The redder and larger circle displayed the more degree connection in the network. The bluer and smaller the circle displayed the less degree connection in the network. The thicker the line and the redder the color, the more degrees were connected in the network. As shown in the network, highly connected clusters were TP53, AKT1, Casp9, Casp8, Casp3, TNF, etc.

DE lncRNA target genes prediction

The top 5 up- and down-regulated differentially expressed lncRNAs were selected for predicting the potential target genes (Table 4). The DE lncRNAs were ENSRNOT00000092009, TCONS_00073996, TCONS_00113453, TCONS_00053590, TCONS_00102805, ENSRNOT00000086889, ENSRNOT00000086208, TCONS_00022155, TCONS_00090467, TCONS_00059568. Their potential target genes, including Fras1, Sim1 and Flrt3, have been reported to be involved in the physiological and pathological functions of immunity, barrier protection and apoptosis.

Table 4 TOP 5 up- and down-regulated DE lncRNAs with potential target genes in G300 VS G0.

LncRNA ID	G300 FPKM	G0 FPKM	Log2FoldChange	Pvalue	Padj	Potential Target Genes
ENSRNOT00000092009	0.00	0.51	-16.97	1.39E-66	2.99E-63	B3galt1
TCONS_00073996	0.00	0.29	-14.90	4.59E-51	1.57E-48	AABR07031918.1, LOC102554034
TCONS_00113453	0.00	0.42	-14.77	3.94E-50	1.18E-47	Sel1l2, Flrt3, AABR07054000.1
TCONS_00053590	0.00	0.27	-14.51	3.43E-48	8.21E-46	Fras1, Mrpl1
TCONS_00102805	0.00	0.44	-14.08	5.84E-45	9.67E-43	Ppp6c, Scai
ENSRNOT00000086889	48.01	0.00	17.28	6.90E-69	1.82E-65	AABR07015525.1
ENSRNOT00000086208	6.53	0.00	16.73	9.70E-65	1.44E-61	Sim1
TCONS_00022155	4.27	0.00	16.29	1.93E-61	1.99E-58	Smim23
TCONS_00090467	3.47	0.00	15.90	1.47E-58	1.16E-55	Srek1
TCONS_00059568	0.28	0.00	15.52	1.10E-55	5.89E-53	AABR07017045.1

Real-Time quantitative PCR analysis

In order to verify the repeatability and reliability of lncRNAs identified by transcriptome sequencing, we randomly selected four lncRNAs from Table 4, namely TCONS_00053590, TCONS_00113453, ENSRNOT00000086889 and ENSRNOT00000086208, for RT-qPCR analysis (Figure 8A). Several of their potential target genes, which contained Flrt3, Fras1, Mrpl1, Sim1, were also verified by RT-qPCR analysis (Figure 8B). The above mentioned lncRNAs and mRNAs, which were potentially important targets for apoptosis regulation at the intersection of the network graph, have also been verified (Figure 8C-D). GAPDH was used as an internal control and relative quantity of expression (fold change). Each lncRNA or mRNA was calculated with the comparative $2^{-\Delta\Delta CT}$ method and the results were consistent with the sequencing data. Values of RT-qPCR shown were mean with Mean±SD. Each RT-qPCR validation was repeated three times. The results showed that these RNAs showed significant differential expression, and was consistent with the change of transcriptome sequencing, indicating that the transcriptome sequencing was reliable.

Discussion

Diabetic gastrointestinal autonomic neuropathy is a common complication of diabetes mellitus. The delayed gastric emptying caused by diabetic gastrointestinal autonomic neuropathy will make the caloric intake and absorption of diabetic patients difficult to match with insulin secretion, which will have adverse effects on blood glucose control[42]and may be a potential mechanism for the development of brittle diabetes[43]. The damage of the ENS in diabetic patients has been proved to be closely related to diabetic gastrointestinal autonomic neuropathy[6, 7]. Studies have shown that ENS is particularly vulnerable to hyperglycemia[44]. When the blood glucose fluctuates obviously (brittle hyperglycemia) or hyperglycemia continues, glucose metabolism in cells changes, which leads to the formation of

advanced glycation end products. This eventually leads to cell damage and cell death through oxidative stress, inflammation and other pathways, which is often referred to as glucose neurotoxicity[45–47].

As an important part of the ENS, EGCs have been proved to play an important role in the occurrence and development of gastrointestinal dysfunction[5, 9, 10]. EGCs can protect neurons by releasing reduced glutathione and glial cell-derived neurotrophic factor (GDNF) under hyperglycemia activation[48, 49]. However, when EGCs apoptosis through oxidative stress and other pathways, the protective effect of EGCs on neurons is weakened[48]. Lopes et al. observed a reduction of the number of EGCs decreased in intermuscular and submucosal plexus in the diabetic rats[6]. It has been shown that EGCs begin to proliferate in the ileum of diabetic mice 4 weeks after the model establishment. The number of EGCs decreased after 8 weeks compared with 4 weeks[28]. However, few articles clearly reveal the mechanism of EGC apoptosis induced by hyperglycemia. In this study, we found G300 treatment could obviously induce cytotoxicity and cell apoptosis; thus G300 was selected as induced concentration to further perform transcriptome analysis.

Increasing evidence has shown that lncRNAs are key mediators in the pathogenesis of diabetes mellitus and its complications[50, 51]. LncRNA-ANRIL participates in the development of diabetes mellitus by promoting β-cell proliferation and inhibiting the expression of CDKN2A. CDKN2A is the key regulator of CREB induced hepatic gluconeogenesis[52, 53]. Li et al. confirmed that lncRNA-Sox2OT gene knockout can protect retinal ganglion cells from hyperglycemia-induced injury and play a neuroprotective role in diabetic retinopathy[54]. LncRNA-MALAT1 has been reported to be involved in the pathogenesis of diabetes and its complications[55]. You et al. have found that downregulation of lncRNA-Meg3 affects Insulin synthesis and secretion in mouse pancreatic β cells [56]. However, the role of lncRNAs in EGCs under hyperglycemia has not been reported. In this study, the involvement of lncRNAs in EGCs under hyperglycemia was analyzed using transcriptome analysis. To reveal the potential function of lncRNAs, their target genes were predicted in Cis in this study. Cis acting lncRNAs regulate gene expression in a manner dependent on their own transcriptional sites[57, 58]. Cis acting lncRNAs have been proved to inhibit, activate or via other mechanisms to regulate the expression of target genes[59–61]. Bioinformatics analysis of lncRNAs target genes in cis suggested that they may participate in some important KEGG pathways, such as T cell receptor signaling pathway, MAPK signaling pathway and Gap junction. Sauer et al. found that T cell receptor signaling can regulate cell function via PI3K/Akt/mTOR pathways[62], which can mediate cell apoptosis as well. It was confirmed by Chyuan et al. that Tumor necrosis factor-related apoptosis-inducing ligand (TRAIL), a ligand which can induce cell apoptosis by transducing apoptosis signals after interacting with its receptor (TRAIL-R), can inhibit T cell activation and inflammatory response through T cell receptor signal pathway[41]. MAPK signaling pathway has been known as one of the key pathways regulating apoptosis[30, 63, 64]. Du et al. found that inhibition of gap junctional communication can induce cardiomyocyte apoptosis through the mitochondrial pathway[65]. Another study showed that interference of gap junctional communication can induce the formation of ovarian reactive oxygen species and further mediate cell apoptosis[66].

Further, Table 3 showed the expression of DE mRNAs and DE lncRNA target genes in apoptosis related KEGG pathways. 19 KEGG pathways were shown in the table. Co-expressed targets, such as Bcl2, Bax, TP53, Casp9, Casp3 and TNF, are widely believed to be involved in apoptosis regulation. And the target genes of DE lncRNAs related KEGG apoptosis pathway were mapped into PPI (Fig. 7). It has been found that TRADD, the key adaptor molecule of TNF-α signal transduction, plays a key role in the regulation of NF-κB[67]. TRADD is a key signal intermediate connecting TNF-α and NF-κB activation. TRADD adaptor protein binds to the death domain of the receptor, and then forms a multi-protein complex. Finally, it leads to the phosphorylation of IkBα, which makes NF-κB transport to the nucleus and stimulates cytokine transcription[68]. As well, TRADD was found to mediates islet β cell apoptosis in diabetes[69, 70]. BIRC family, also known as the inhibitor of apoptosis proteins (IAPs), consists of eight members[71]. BIRC2 and BIRC3 proteins indirectly regulate caspase activation through E3 ligase activity, TNF signal transduction and NF-kB signal transduction[72–75]. Through the analysis of TNF-α protein network, Jamil et al. found that TNF-mediated proteins BIRC2 and BIRC3 were involved in the pathogenesis of T2DM[76]. RelA/p65 is considered to be a key subunit of NF-κB signal transduction, which is a key target of mitochondrial metabolism and apoptosis[77]. A large number of studies have shown that diabetes and its complications, such as diabetic retinopathy, diabetic nephropathy and diabetic peripheral neuropathy, are partly through the deacetylation of RelA/p65, which is related to the pathogenesis of the disease[78–80]. Wang et al. proved that catalase can partly improve diabetes induced autophagy by increasing the activity of NF-κB pathway and BECN1 transcription mediated by RelA/p65(Wang et al., 2017).

It was known that the regulatory networks of lncRNAs, miRNAs, and mRNAs, also called competing endogenous RNAs (ceRNAs), communicated with each other to regulate gene expression[81]. Studies suggested that ceRNAs can regulate the occurrence and development of diabetes and its complications through protein synthesis, ER stress, RNA binding and protein translation[82]. Li et al. have shown that targeted ceRAN is involved in the regulation of apoptosis induced by hyperglycemia, which provides a new treatment strategy for diabetes and its complications(Li et al., 2016).

In this study, several DE lncRNAs and mRNAs were at the key junction points of the regulatory network. TCONS_00012166-miR-362-5p-ENSRNOG00000046202 (Metrnl) axis was found to be up-down-up change. Metrnl is a recently discovered adipokine highly expressed in subcutaneous adipose tissue[40], which contains functions such as promoting nerve development[84], regulating the immune system and so on[85, 86]. It can regulate triglyceride, cholesterol, low density lipoprotein, high density lipoprotein and other blood lipid components[87]. Chung et al. demonstrated that in human subjects with T2DM, Metrnl levels were elevated and negatively correlated with various metabolic risk factors[88], which has been proved to work by antagonizing insulin resistance through multiple signaling pathways[89, 90]. TCONS_00083285-miR-187-3p-ENSRNOG00000018233 (Gas6) axis was found to be down-up-down change. Growth arrest specific-6 (Gas6) can be linked to phosphatidylserine on the surface of apoptotic cells, thus triggering effector cell action[91]. Nepal et al. found that macrophages can remove apoptotic neutrophils and eliminate inflammation by inducing Gas6 expression[92]. In addition, we selected 5 mRNAs and 5 lncRNAs at the intersection of the network graph and verified them by RT-qPCR (Fig. 8C-D).

As shown in the Table 4, we screened out the top 5 up- and down-regulated DE lncRNAs with potential target genes. FLRT3, an axon guidance-related factor, has been found to be related to the regulation of nerve cell growth and morphogenesis[93]. FLRT3 has been proved to regulate the growth of nerve cells after peripheral nerve injury[94, 95]. In our results, TCONS_00113453 was significantly down-regulated in G300 group. It can promote the repair of nervous system damage and the growth of synapse by regulating potential target gene FLRT3. FRAS1 is related to the regulation of extracellular matrix composition, maintenance of basement membrane integrity, epithelial adhesion and signal transduction[96, 97]. Nikolova et al. reported that FRAS1-related extracellular matrix 3 (FREM3)[98] may participate in cell-cell interaction and maintain the structural and functional integrity of nerve tissue. As shown in our results, TCONS_00053590 may up-regulated its potential target gene FRAS1 through down regulation in G300 group, which may play a role in extracellular matrix regulation and neuronal protection. In our study, the expression changes of randomly selected lncRNAs and several potential target mRANs have been verified by RT-qPCR (Fig. 8A-B), showed a strong correlation with that identified with RNA-Seq.

Conclusion

In conclusion, RNA-Seq of the lncRNAs in EGCs under hyperglycemia revealed that totally 4678 DE lncRNAs and 6244 DE mRNAs were obtained according to the fold change ≥ 2 and padj < 0.05. And 1383 DE lncRNAs, 3234 DE mRNAs were down-regulated, whereas 3295 and 3010 were up-regulated in G300 group compared to G0 group. These DE lncRNAs and DE mRNAs were affected by hyperglycemia in EGCs and which influenced EGCs function. Clarifying the relationship between lncRNAs and EGCs under hyperglycemia may be helpful for understanding the pathogenesis of diabetes and provide new therapeutic strategy for diabetic gastrointestinal autonomic neuropathy.

Declarations

Funding

This work was approved and funded by the Young Talent's Subsidy Project in Science and Education of the Department of Public Health of Jiangsu Province (No. QNRC2016627), Six talent peaks project in Jiangsu Province (No. WSW-047), Six-one Scientific Research Project (No. LGY2019087), Wuxi health commission (No. M202011).

Data availability statement

The RNA-Seq Bioproject data are accessible at the SRA of National Center for Biotechnology Information (NCBI) Bioproject under accession number PRJNA660192.

Author contributions

Lan Xu and Ke Wang conceived, designed and coordinated the experiments; Xuping Zhu and Yanyu Li drafted and wrote the manuscript; Xue Zhu, Yanmin Jiang and Xiaowei Zhu revised and revised the manuscript; Xiang Xu, Chao Liu and Chengming Ni analyzed and sorted out the data. All authors have read and agreed to the published version of the manuscript.

Ethics approval

Not applicable.

Consent for publication

Not applicable.

Conflicts of interest

The authors declare no conflicts of interest.

Acknowledge

Not applicable.

References

1. Lovic D, Piperidou A, Zografou I, Grassos H, Pittaras A, Manolis A. The Growing Epidemic of Diabetes Mellitus. Curr Vasc Pharmacol. 2020;18:104–9.
2. Ogurtsova K, da Rocha Fernandes JD, Huang Y, Linnenkamp U, Guariguata L, Cho NH, et al. IDF Diabetes Atlas: Global estimates for the prevalence of diabetes for 2015 and 2040. Diabetes Res Clin Pract. 2017;128:40–50.
3. Yarandi SS, Srinivasan S. Diabetic gastrointestinal motility disorders and the role of enteric nervous system: Current status and future directions. Neurogastroenterol Motil. 2014;26:611–24.
4. Chedid V, Brandler J, Vijayvargiya P, Park SY, Szarka LA, Camilleri M. Characterization of Upper Gastrointestinal Symptoms, Gastric Motor Functions, and Associations in Patients with Diabetes at a Referral Center. Am J Gastroenterol. 2019;114:143–54.
5. Brock C, Softeland E, Gunterberg V, Frokjaer JB, Lelic D, Brock B, et al. Diabetic Autonomic Neuropathy Affects Symptom Generation and Brain-Gut Axis. Diabetes Care. 2013;36:3698–705.
6. Lopes CRP, Ferreira PEB, Zanoni JN, Alves AMP, Alves ÉPB, Buttow NC. Neuroprotective Effect of Quercetin on the Duodenum Enteric Nervous System of Streptozotocin-Induced Diabetic Rats. Dig Dis Sci. 2012;57:3106–15.
7. Hermes-Uliana C, Panizzon CPDNB, Trevizan AR, Sehaber CC, Ramalho FV, Martins HA, et al. Is L-glutathione more effective than L-glutamine in preventing enteric diabetic neuropathy? Dig Dis Sci. 2014;59:937–48.

8. Chng SH, Pachnis V. Enteric Nervous System: lessons from neurogenesis for reverse engineering and disease modelling and treatment. Curr Opin Pharmacol. 2020;50:100–6.
9. gomes p., Chevalier J, Boesmans W, Roosen L, van den abbeel V, Neunlist M, et al. ATP-dependent paracrine communication between enteric neurons and glia in a primary cell culture derived from embryonic mice. Neurogastroenterol Motil. 2009;21:870-e62.
10. Du F, Wang L, Qian W, Liu S. Loss of enteric neurons accompanied by decreased expression of GDNF and PI3K/Akt pathway in diabetic rats. Neurogastroenterol Motil. 2009;21:1229–35.
11. Xiao W, Wang W, Chen W, Sun L, Li X, Zhang C, et al. GDNF is Involved in the Barrier-Inducing Effect of Enteric Glial Cells on Intestinal Epithelial Cells Under Acute Ischemia Reperfusion Stimulation. Mol Neurobiol. 2014;50:274–89.
12. Bassotti G, Villanacci V. Can “functional” constipation be considered as a form of enteric neuro-gliopathy? Glia. 2011;59:345–50.
13. Jiang Y, Xu L, Yu L, Xu X, Feng C, Li J. NOX4 inhibition protects enteric glial cells against Clostridium difficile toxin B toxicity via attenuating oxidative and Endoplasmic reticulum stresses. Free Radic Res. 2019;53:932–40.
14. Savidge TC, Newman P, Pothoulakis C, Ruhl A, Neunlist M, Bourreille A, et al. Enteric Glia Regulate Intestinal Barrier Function and Inflammation Via Release of S-Nitrosoglutathione. Gastroenterology. 2007;132:1344–58.
15. Neunlist M, Van Landeghem L, Mahé MM, Derkinderen P, Des Varannes SB, Rolli-Derkinderen M. The digestive neuronal-glial-epithelial unit: A new actor in gut health and disease. Nat Rev Gastroenterol Hepatol. 2013;10:90–100.
16. Alves EPB, Alves AMP, Pereira RVF, Neto MHDM, Zanoni JN. Immunohistochemical study of vasoactive intestinal peptide (VIP) enteric neurons in diabetic rats supplemented with L-glutamine. Nutr Neurosci. 2010;13:43–51.
17. Neunlist M, Aubert P, Bonnaud S, Van Landeghem L, Coron E, Wedel T, et al. Enteric glia inhibit intestinal epithelial cell proliferation partly through a TGF-β 1 -dependent pathway. Am J Physiol Liver Physiol. 2007;292:G231–41.
18. Gulbransen BD, Bains JS, Sharkey KA. Enteric glia are targets of the sympathetic innervation of the myenteric plexus in the guinea pig distal colon. J Neurosci. 2010;30:6801–9.
19. Zeng F, Watson RP, Nash MS. Glial Cell–Derived Neurotrophic Factor Enhances Synaptic Communication and 5-Hydroxytryptamine 3a Receptor Expression in Enteric Neurons. Gastroenterology. 2010;138:1491–501.
20. Xie Q, Chen X, Zhang MM, Huang XL, Zhang Q, Zhou JQ, et al. Glial-derived neurotrophic factor regulates enteric mast cells and ameliorates dextran sulfate sodium-induced experimental colitis. Int Immunopharmacol. 2020;85 October 2019:106638.
21. Guttman M, Rinn JL. Modular regulatory principles of large non-coding RNAs. Nature. 2012;482:339–46.

22. Lu Y, Liu X, Xie M, Liu M, Ye M, Li M, et al. The NF-κB–Responsive Long Noncoding RNA FIRRE Regulates Posttranscriptional Regulation of Inflammatory Gene Expression through Interacting with hnRNPU. J Immunol. 2017;199:3571–82.
23. Motterle A, Gattesco S, Peyot ML, Esguerra JLS, Gomez-Ruiz A, Laybutt DR, et al. Identification of islet-enriched long non-coding RNAs contributing to β-cell failure in type 2 diabetes. Mol Metab. 2017;6:1407–18.
24. Wang X, Chang X, Zhang P, Fan L, Zhou T, Sun K. Aberrant Expression of Long Non-Coding RNAs in Newly Diagnosed Type 2 Diabetes Indicates Potential Roles in Chronic Inflammation and Insulin Resistance. Cell Physiol Biochem. 2017;43:2367–78.
25. Yan C, Chen J, Chen N. Long noncoding RNA MALAT1 promotes hepatic steatosis and insulin resistance by increasing nuclear SREBP-1c protein stability. Sci Rep. 2016;6:22640.
26. Reutens AT, Bonnet F, Lantieri O, Roussel R, Balkau B. The association between cystatin C and incident type 2 diabetes is related to central adiposity. Nephrol Dial Transplant. 2013;28:1820–9.
27. Chen Y, Liu G, He F, Zhang L, Yang K, Yu H, et al. MicroRNA 375 modulates hyperglycemia-induced enteric glial cell apoptosis and Diabetes-induced gastrointestinal dysfunction by targeting Pdk1 and repressing PI3K/Akt pathway. Sci Rep. 2018;8:1–10.
28. Luo P, Liu D, Li C, He WX, Zhang CL, Chang MJ. Enteric glial cell activation protects enteric neurons from damage due to diabetes in part via the promotion of neurotrophic factor release. Neurogastroenterol Motil. 2018;30:1–10.
29. Wu GJ, Chen WF, Hung HC, Jean YH, Sung CS, Chakraborty C, et al. Effects of propofol on proliferation and anti-apoptosis of neuroblastoma SH-SY5Y cell line: New insights into neuroprotection. Brain Res. 2011;1384:42–50.
30. Sun HY, Hu KZ, Yin ZS. Inhibition of the p38-MAPK signaling pathway suppresses the apoptosis and expression of proinflammatory cytokines in human osteoarthritis chondrocytes. Cytokine. 2017;90:135–43.
31. Ruan Y, Lin N, Ma Q, Chen R, Zhang Z, Wen W, et al. Circulating LncRNAs Analysis in Patients with Type 2 Diabetes Reveals Novel Genes Influencing Glucose Metabolism and Islet β-Cell Function. Cell Physiol Biochem. 2018;46:335–50.
32. Deng G, Moran EP, Cheng R, Matlock G, Zhou K, Moran D, et al. Therapeutic effects of a novel agonist of peroxisome proliferator-activated receptor alpha for the treatment of diabetic retinopathy. Investig Ophthalmol Vis Sci. 2017;58:5030–42.
33. Wapinski OL, Vierbuchen T, Qu K, Lee QY, Chanda S, Fuentes DR, et al. XHierarchical mechanisms for direct reprogramming of fibroblasts to neurons. Cell. 2013;155:621.
34. Jia Y, Shi L, Yun F, Liu X, Chen Y, Wang M, et al. Transcriptome sequencing profiles reveal lncRNAs may involve in breast cancer (ER/PR positive type) by interaction with RAS associated genes. Pathol Res Pract. 2019;215:152405.
35. Manley LJ, Ma D, Levine SS. Monitoring error rates in Illumina sequencing. J Biomol Tech. 2016;27:125–8.

36. Dobin A, Davis CA, Schlesinger F, Drenkow J, Zaleski C, Jha S, et al. STAR: ultrafast universal RNA-seq aligner. Bioinformatics. 2013;29:15–21.
37. Ferreira JA, Zwinderman AH. On the Benjamini-Hochberg method. Ann Stat. 2006;34:1827–49.
38. Chen W, Chen X, Wang Y, Liu T, Liang Y, Xiao Y, et al. Construction and analysis of lncRNA-Mediated ceRNA network in cervical squamous cell carcinoma by weighted gene Co-Expression network analysis. Med Sci Monit. 2019;25:2609–22.
39. Zhou HQ, Chen QC, Qiu ZT, Tan WL, Mo CQ, Gao SW. Integrative microRNA-mRNA and protein-protein interaction analysis in pancreatic neuroendocrine tumors. Eur Rev Med Pharmacol Sci. 2016;20:2842–52.
40. Li ZY, Zheng SL, Wang P, Xu TY, Guan YF, Zhang YJ, et al. Subfatin is a Novel Adipokine and Unlike Meteorin in Adipose and Brain Expression. CNS Neurosci Ther. 2014;20:344–54.
41. Chyuan IT, Tsai HF, Wu CS, Sung CC, Hsu PN. TRAIL-mediated suppression of T cell receptor signaling inhibits T cell activation and inflammation in experimental autoimmune encephalomyelitis. Front Immunol. 2018;9 JAN:1–14.
42. Camilleri M, McCallum RW, Tack J, Spence SC, Gottesdiener K, Fiedorek FT. Efficacy and Safety of Relamorelin in Diabetics With Symptoms of Gastroparesis: A Randomized, Placebo-Controlled Study. Gastroenterology. 2017;153:1240–1250.e2.
43. Horváth VJ, Izbéki F, Lengyel C, Kempler P, Várkonyi T. Diabetic gastroparesis: Functional/morphologic background, diagnosis, and treatment options. Curr Diab Rep. 2014;14:1–9.
44. Meldgaard T, Olesen SS, Farmer AD, Krogh K, Wendel AA, Brock B, et al. Diabetic enteropathy: From molecule to mechanism-based treatment. J Diabetes Res. 2018;2018.
45. Meldgaard T, Keller J, Olesen AE, Olesen SS, Krogh K, Borre M, et al. Pathophysiology and management of diabetic gastroenteropathy. Therap Adv Gastroenterol. 2019;12:1–17.
46. Bulc M, Palus K, Całka J, Zielonka L. Changes in Immunoreactivity of Sensory Substances within the Enteric Nervous System of the Porcine Stomach during Experimentally Induced Diabetes. J Diabetes Res. 2018;2018.
47. Kempler P, Várkonyi T, Körei AE, Horváth VJ. Gastrointestinal autonomic neuropathy in diabetes: the unattended borderline between diabetology and gastroenterology. Diabetologia. 2016;59:401–3.
48. Vergnolle N, Cirillo C. Neurons and Glia in the Enteric Nervous System and Epithelial Barrier Function. Physiology. 2018;33:269–80.
49. Wang Z, Ocadiz-Ruiz R, Sundaresan S, Ding L, Hayes M, Sahoo N, et al. Isolation of Enteric Glial Cells from the Submucosa and Lamina Propria of the Adult Mouse. J Vis Exp. 2018;:1–11.
50. Motterle A, Gattesco S, Peyot M, Esguerra JLS, Gomez-Ruiz A, Laybutt DR, et al. Identification of islet-enriched long non-coding RNAs contributing to β-cell failure in type 2 diabetes. Mol Metab. 2017;6:1407–18.
51. Feng SD, Yang JH, Yao CH, Yang SS, Zhu ZM, Wu D, et al. Potential regulatory mechanisms of lncRNA in diabetes and its complications. Biochem Cell Biol. 2017;95:361–7.

52. Duesing K, Fatemifar G, Charpentier G, Marre M, Tichet J, Hercberg S, et al. Strong association of common variants in the CDKN2A/CDKN2B region with type 2 diabetes in French Europids. Diabetologia. 2008;51:821–6.
53. Rong R, Hanson RL, Ortiz D, Wiedrich C, Kobes S, Knowler WC, et al. Association Analysis of Variation in/Near FTO, CDKAL1, SLC30A8, HHEX, EXT2, IGF2BP2, LOC387761, and CDKN2B With Type 2 Diabetes and Related Quantitative Traits in Pima Indians. Diabetes. 2009;58:478–88.
54. Li C-P, Wang S-H, Wang W-Q, Song S-G, Liu X-M. Long Noncoding RNA-Sox2OT Knockdown Alleviates Diabetes Mellitus-Induced Retinal Ganglion Cell (RGC) injury. Cell Mol Neurobiol. 2017;37:361–9.
55. Liu JY, Yao J, Li XM, Song YC, Wang XQ, Li YJ, et al. Pathogenic role of lncRNA-MALAT1 in endothelial cell dysfunction in diabetes mellitus. Cell Death Dis. 2014;5:e1506–e1506.
56. You L, Wang N, Yin D, Wang L, Jin F, Zhu Y, et al. Downregulation of Long Noncoding RNA Meg3 Affects Insulin Synthesis and Secretion in Mouse Pancreatic Beta Cells. J Cell Physiol. 2016;231:852–62.
57. Gil N, Ulitsky I. Regulation of gene expression by cis-acting long non-coding RNAs. Nat Rev Genet. 2020;21:102–17.
58. Ding M, Liu Y, Liao X, Zhan H, Liu Y, Huang W. Enhancer RNAs (eRNAs): New Insights into Gene Transcription and Disease Treatment. J Cancer. 2018;9:2334–40.
59. Chen H, Du G, Song X, Li L. Non-coding Transcripts from Enhancers: New Insights into Enhancer Activity and Gene Expression Regulation. Genomics, Proteomics Bioinforma. 2017;15:201–7.
60. Li W, Notani D, Rosenfeld MG. Enhancers as non-coding RNA transcription units: Recent insights and future perspectives. Nat Rev Genet. 2016;17:207–23.
61. Nozawa RS, Boteva L, Soares DC, Naughton C, Dun AR, Buckle A, et al. SAF-A Regulates Interphase Chromosome Structure through Oligomerization with Chromatin-Associated RNAs. Cell. 2017;169:1214–1227.e18.
62. Sauer S, Bruno L, Hertweck A, Finlay D, Leleu M, Spivakov M, et al. T cell receptor signaling controls Foxp3 expression via PI3K, Akt, and mTOR. Proc Natl Acad Sci. 2008;105:7797–802.
63. Sun QY, Ding LW, Johnson K, Zhou S, Tyner JW, Yang H, et al. SOX7 regulates MAPK/ERK-BIM mediated apoptosis in cancer cells. Oncogene. 2019;38:6196–210.
64. Li D, Yang M, Liao A, Zeng B, Liu D, Yao Y, et al. Linc00483 as ceRNA regulates proliferation and apoptosis through activating MAPKs in gastric cancer. J Cell Mol Med. 2018;22:3875–86.
65. Du ZJ, Cui GQ, Zhang J, Liu XM, Zhang ZH, Jia Q, et al. Inhibition of gap junction intercellular communication is involved in silica nanoparticles-induced H9c2 cardiomyocytes apoptosis via the mitochondrial pathway. Int J Nanomedicine. 2017;12:2179–88.
66. López-Arellano P, López-Arellano K, Luna J, Flores D, Jiménez-Salazar J, Gavia G, et al. Perfluorooctanoic acid disrupts gap junction intercellular communication and induces reactive oxygen species formation and apoptosis in mouse ovaries. Environ Toxicol. 2019;34:92–8.

67. Wang H, Cebotaru L, Lee HW, Yang Q, Pollard BS, Pollard HB, et al. CFTR Controls the Activity of NF-κB by Enhancing the Degradation of TRADD. Cell Physiol Biochem. 2016;40:1063–78.
68. Pobezinskaya YL, Liu Z. The role of TRADD in death receptor signaling. Cell Cycle. 2012;11:871–6.
69. Rojas J, Bermudez V, Palmar J, Martínez MS, Olivar LC, Nava M, et al. Pancreatic Beta Cell Death: Novel Potential Mechanisms in Diabetes Therapy. J Diabetes Res. 2018;2018 Dm:1–19.
70. Weir GC, Ehlers MR, Harris KM, Kanaparthi S, Long A, Phippard D, et al. Alpha-1 antitrypsin treatment of new-onset type 1 diabetes: An open-label, phase I clinical trial (RETAIN) to assess safety and pharmacokinetics. Pediatr Diabetes. 2018;19:945–54.
71. Hrdinka M, Yabal M. Inhibitor of apoptosis proteins in human health and disease. Genes Immun. 2019;20:641–50.
72. Asslaber D, Wacht N, Leisch M, Qi Y, Maeding N, Hufnagl C, et al. BIRC3 expression predicts CLL progression and defines treatment sensitivity via enhanced NF-kB nuclear translocation. Clin Cancer Res. 2019;25:1901–12.
73. Eytan DF, Snow GE, Carlson S, Derakhshan A, Saleh A, Schiltz S, et al. SMAC mimetic birinapant plus radiation eradicates human head and neck cancers with genomic amplifications of cell death genes FADD and BIRC2. Cancer Res. 2016;76:5442–54.
74. Ebner P, Poetsch I, Deszcz L, Hoffmann T, Zuber J, Ikeda F. The IAP family member BRUCE regulates autophagosome–lysosome fusion. Nat Commun. 2018;9:1–15.
75. Lee JY, Tokumoto M, Hwang GW, Lee MY, Satoh M. Identification of ARNT-regulated BIRC3 as the target factor in cadmium renal toxicity. Sci Rep. 2017;7:1–16.
76. Jamil K, Jayaraman A, Ahmad J, Joshi S, Yerra SK. TNF-alpha – 308G/A and – 238G/A polymorphisms and its protein network associated with type 2 diabetes mellitus. Saudi J Biol Sci. 2017;24:1195–203.
77. Ivanova IG, Perkins ND. Hypoxia induces rapid, STAT3 and ROS dependent, mitochondrial translocation of RelA(p65) and IκBα. Biosci Rep. 2019;39:1–13.
78. Feng Y, Chen L, Luo Q, Wu M, Chen Y, Shi X. Involvement of microRNA-146a in diabetic peripheral neuropathy through the regulation of inflammation. Drug Des Devel Ther. 2018;12:171–7.
79. Wang X, Tao Y, Huang Y, Zhan K, Xue M, Wang Y, et al. Catalase ameliorates diabetes-induced cardiac injury through reduced p65/RelA- mediated transcription of BECN1. J Cell Mol Med. 2017;21:3420–34.
80. Zhong Y, Lee K, He JC. SIRT1 is a potential drug target for treatment of diabetic kidney disease. Front Endocrinol (Lausanne). 2018;9 OCT:1–6.
81. Yu S, Zhao Y, Lai F, Chu M, Hao Y, Feng Y, et al. LncRNA as ceRNAs may be involved in lactation process. Oncotarget. 2017;8:98014–28.
82. Kato M, Wang M, Chen Z, Bhatt K, Oh HJ, Lanting L, et al. An endoplasmic reticulum stress-regulated lncRNA hosting a microRNA megacluster induces early features of diabetic nephropathy. Nat Commun. 2016;7:12864.

83. Li X, Wang H, Yao B, Xu W, Chen J, Zhou X. LncRNA H19/miR-675 axis regulates cardiomyocyte apoptosis by targeting VDAC1 in diabetic cardiomyopathy. Sci Rep. 2016;6 October:1–9.
84. Jørgensen JR, Fransson A, Fjord-Larsen L, Thompson LH, Houchins JP, Andrade N, et al. Cometin is a novel neurotrophic factor that promotes neurite outgrowth and neuroblast migration in vitro and supports survival of spiral ganglion neurons in vivo. Exp Neurol. 2012;233:172–81.
85. Ushach I, Arrevillaga-Boni G, Heller GN, Pone E, Hernandez-Ruiz M, Catalan-Dibene J, et al. Meteorin-like/Meteorin-β Is a Novel Immunoregulatory Cytokine Associated with Inflammation. J Immunol. 2018;201:3669–76.
86. Zheng SL, Li ZY, Song J, Liu JM, Miao CY. Metrnl: A secreted protein with new emerging functions. Acta Pharmacol Sin. 2016;37:571–9.
87. Qi Q, Hu W jun, Zheng S li, Zhang S long, Le Y ying, Li Z yong, et al. Metrnl deficiency decreases blood HDL cholesterol and increases blood triglyceride. Acta Pharmacol Sin. 2020; October 2019:1–8.
88. Chung HS, Hwang SY, Choi JH, Lee HJ, Kim NH, Yoo HJ, et al. Implications of circulating Meteorin-like (Metrnl) level in human subjects with type 2 diabetes. Diabetes Res Clin Pract. 2018;136:100–7.
89. Li ZY, Song J, Zheng SL, Fan MB, Guan YF, Qu Y, et al. Adipocyte metrnl antagonizes insulin resistance through pparg signaling. Diabetes. 2015;64:4011–22.
90. Wang K, Li F, Wang C, Deng Y, Cao Z, Cui Y, et al. Serum levels of meteorin-like (Metrnl) are increased in patients with newly diagnosed type 2 diabetes mellitus and are associated with insulin resistance. Med Sci Monit. 2019;25:2337–43.
91. Van Der Meer JHM, Van Der Poll T, Van't Veer C. TAM receptors, Gas6, and protein S: Roles in inflammation and hemostasis. Blood. 2014;123:2460–9.
92. Nepal S, Tiruppathi C, Tsukasaki Y, Farahany J, Mittal M, Rehman J, et al. STAT6 induces expression of Gas6 in macrophages to clear apoptotic neutrophils and resolve inflammation. Proc Natl Acad Sci. 2019;116:16513–8.
93. Leyva-Díaz E, del Toro D, Menal MJ, Cambray S, Susín R, Tessier-Lavigne M, et al. FLRT3 Is a Robo1-Interacting Protein that Determines Netrin-1 Attraction in Developing Axons. Curr Biol. 2014;24:494–508.
94. Yamagishi S, Hampel F, Hata K, Del Toro D, Schwark M, Kvachnina E, et al. FLRT2 and FLRT3 act as repulsive guidance cues for Unc5-positive neurons. EMBO J. 2011;30:2920–33.
95. Robinson M, Parsons Perez MC, Tébar L, Palmer J, Patel A, Marks D, et al. FLRT3 is expressed in sensory neurons after peripheral nerve injury and regulates neurite outgrowth. Mol Cell Neurosci. 2004;27:202–14.
96. Miller KA, Gordon CT, Welfare MF, Caruana G, Bertram JF, Bateman JF, et al. bfb, a Novel ENU-Induced blebs Mutant Resulting from a Missense Mutation in Fras1. PLoS One. 2013;8:e76342.
97. Wiradjaja F, Cottle DL, Jones L, Smyth I. Regulation of PDGFC signalling and extracellular matrix composition by FREM1 in mice. DMM Dis Model Mech. 2013;6:1426–33.

98. Nikolova YS, Iruku SP, Lin C-W, Conley ED, Puralewski R, French B, et al. FRAS1-related extracellular matrix 3 (FREM3) single-nucleotide polymorphism effects on gene expression, amygdala reactivity and perceptual processing speed: An accelerated aging pathway of depression risk. Front Psychol. 2015;6 September:1–15.

Figures

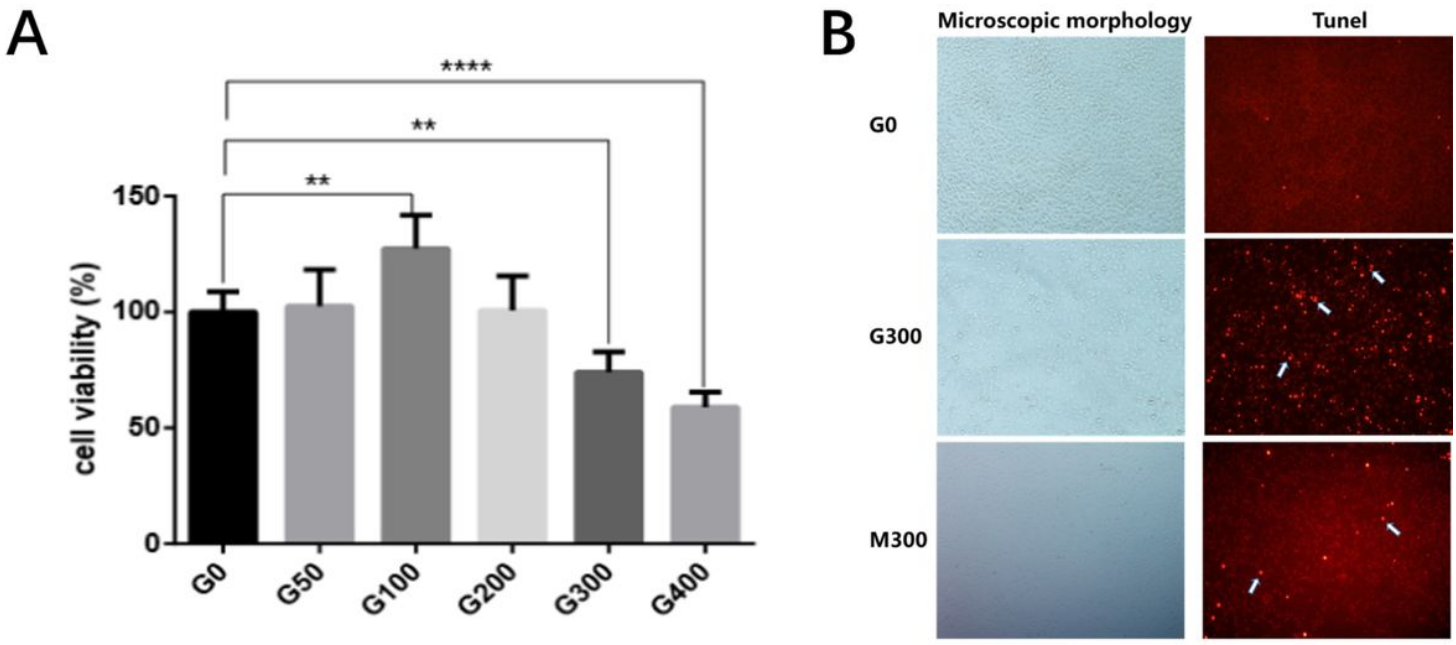

Figure 1

Apoptosis of EGCs under hyperglycemia induction. (A) MTT assay of EGCs at different glucose concentrations. (B) Left was microscopic morphology of G0, G300 and M300. Right was Tunel assay for apoptotic cells.

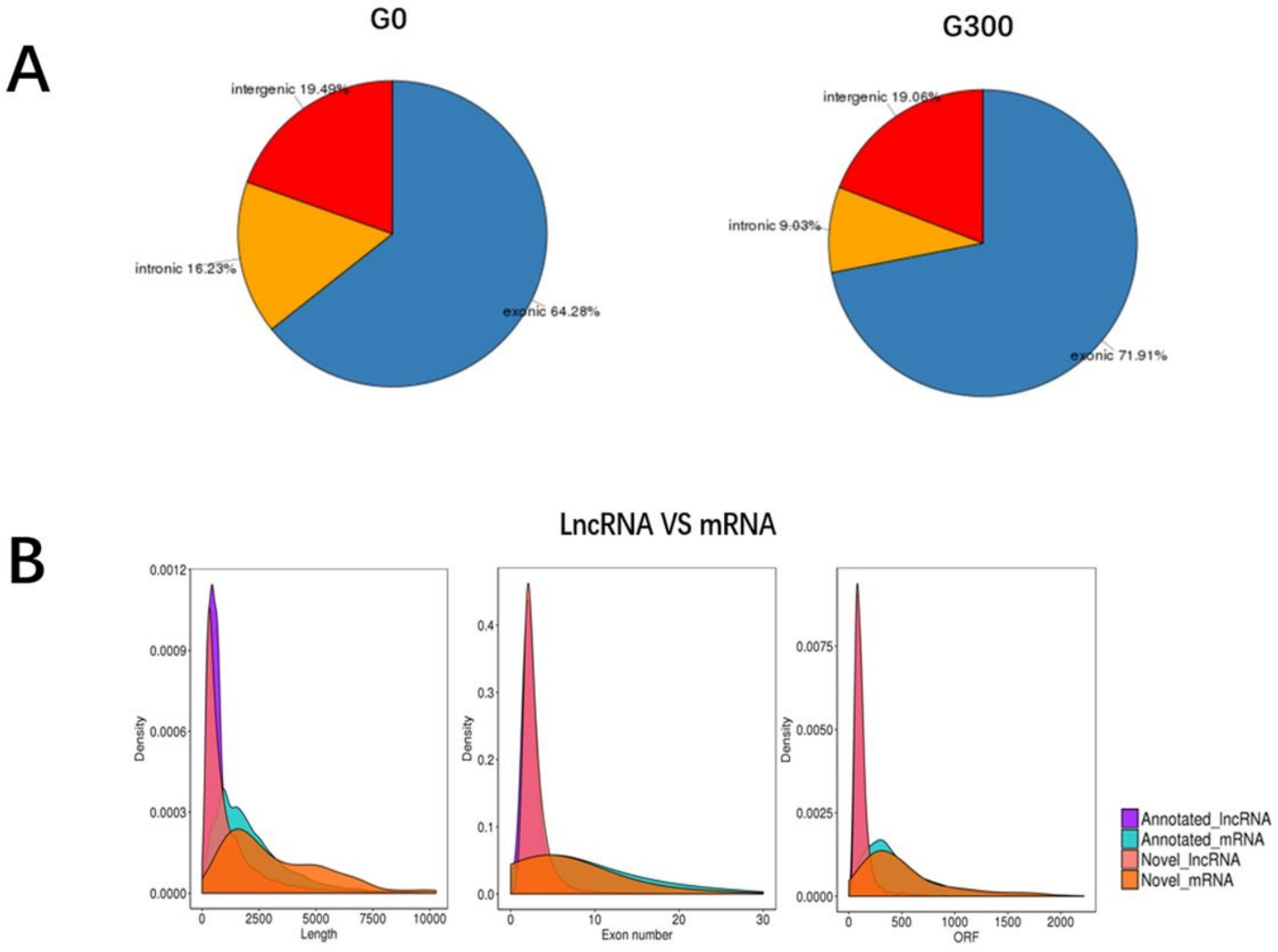

Figure 2

(A) The percent of reads to genome regions. (B) Transcript length, exon number and ORF of lncRNAs and mRNAs. The purple region represents annotated lncRNAs, and the red region represents the novel lncRNAs. The cyan region represents annotated mRNAs, and the orange region represents novel lncRNAs.

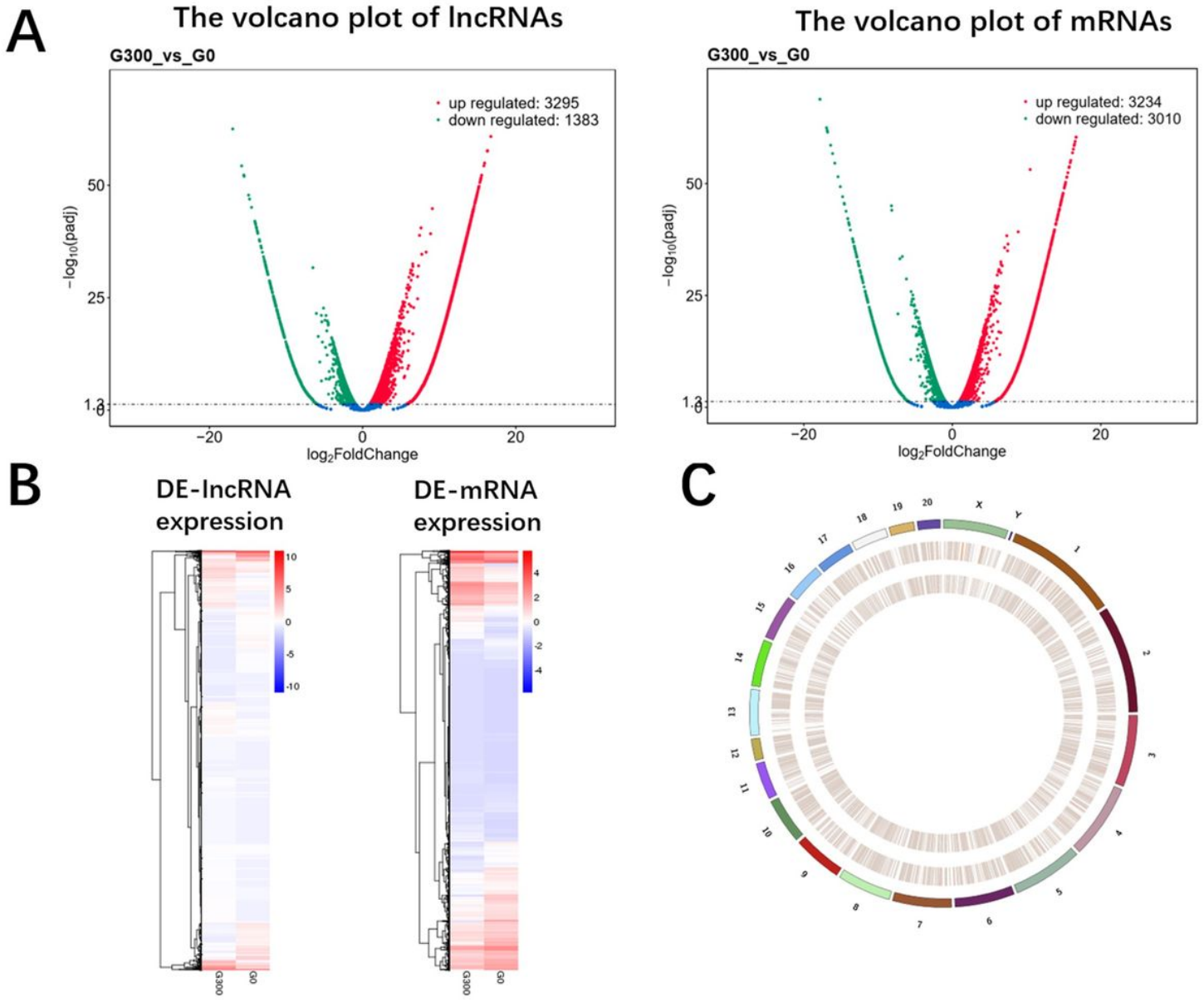

Figure 3

Differential expression of lncRNAs and mRNAs in G0 and G300. (A) Volcano plots of the differentially expressed lncRNAs and mRNAs in G0 and G300. (B) Hierarchical clustering of a subset of the differentially expressed lncRNAs and mRNAs. (C) Circus plot representation of lncRNAs and mRNAs on the basis of their expression.

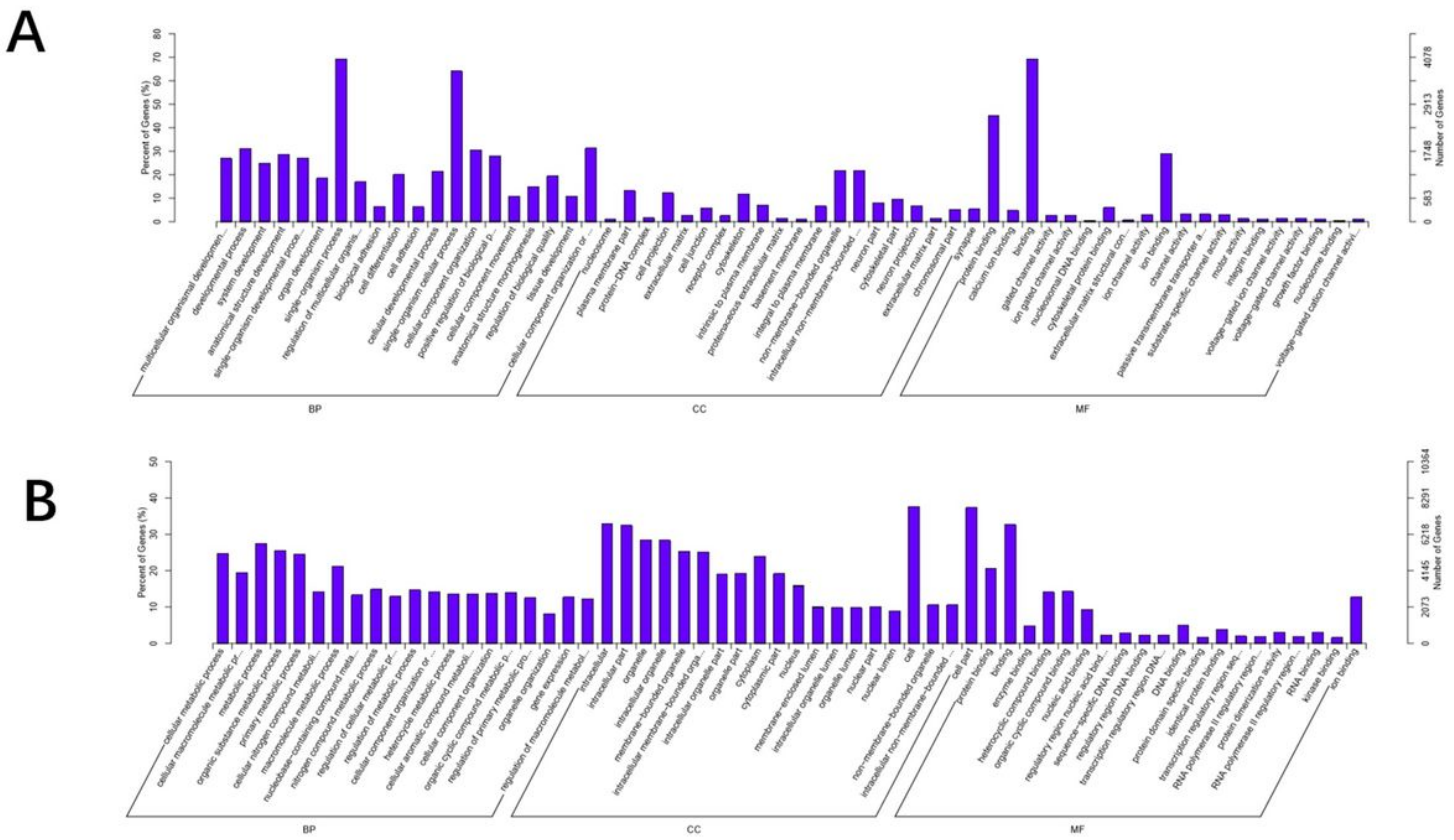

Figure 4

| GO terms which enriched the DEGs and DE lncRNA target genes. BP is short for biological; CC is short for cellular; MF is short for molecular function. (A) GO enrichment analysis of DEGs. (B) GO enrichment analysis of DE lncRNA target genes.

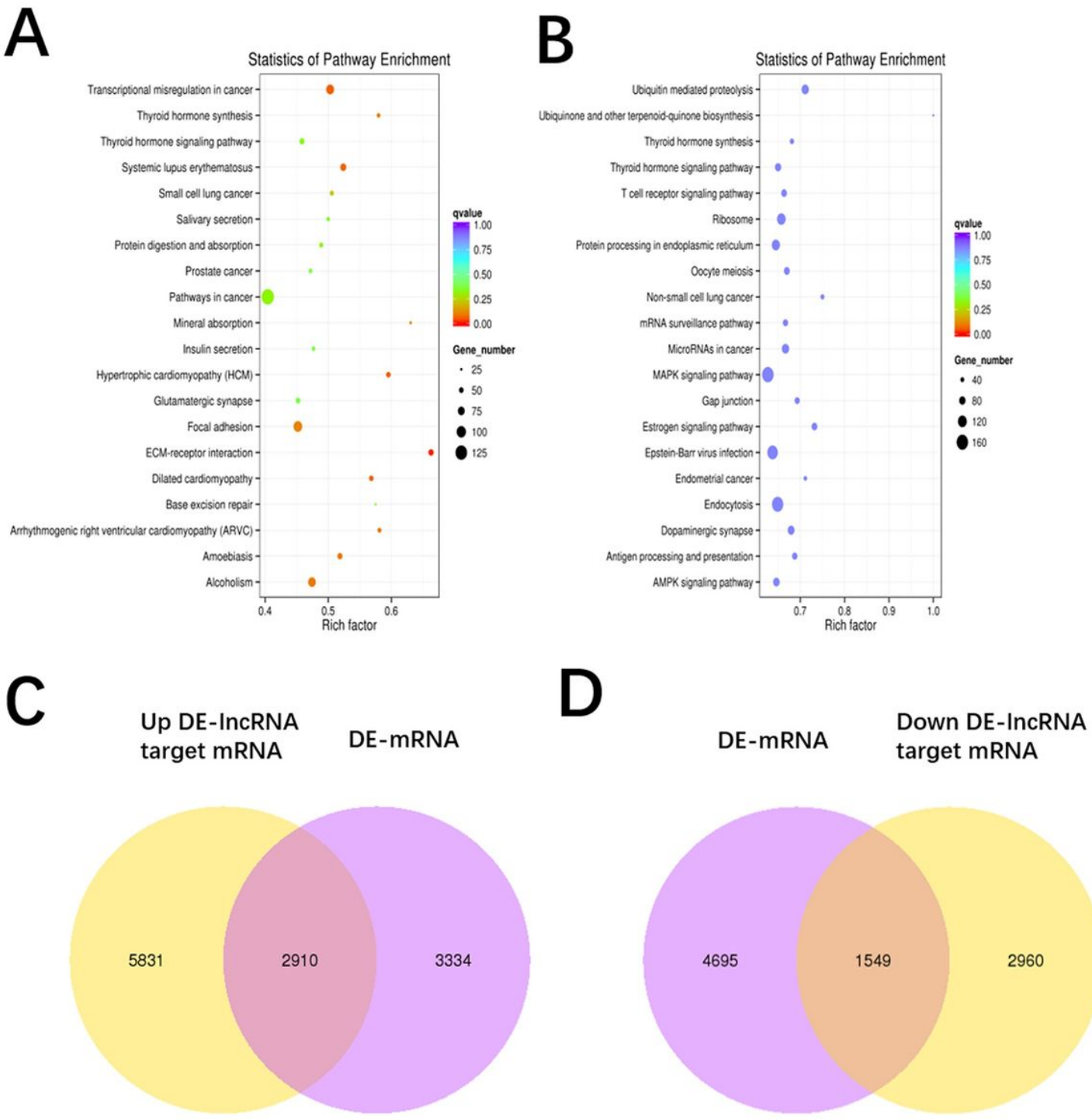

Figure 5

Scatter plots of KEGG pathway enrichment and Venn diagrams of DE mRNAs and DE lncRNA target genes. (A) The top 20 enriched KEGG pathways resulted from the DE mRNAs significantly regulated genes. The ordinate represents different pathways, and the abscissa represents the proportion of the differentially expressed genes in the corresponding pathways. The size of the circle represents the number of genes enriched in the corresponding pathway, and the larger the circle, the more genes are enriched in the corresponding pathway. Color represents enrichment significance, and the closer to red,

the more significant. (B) The top 20 enriched KEGG pathways resulted from the DE lncRNA target genes. (C) Venn diagram of DE mRNAs and up DE lncRNA target mRNAs. (D) Venn diagram of DE mRNAs and down DE lncRNA target mRNAs.

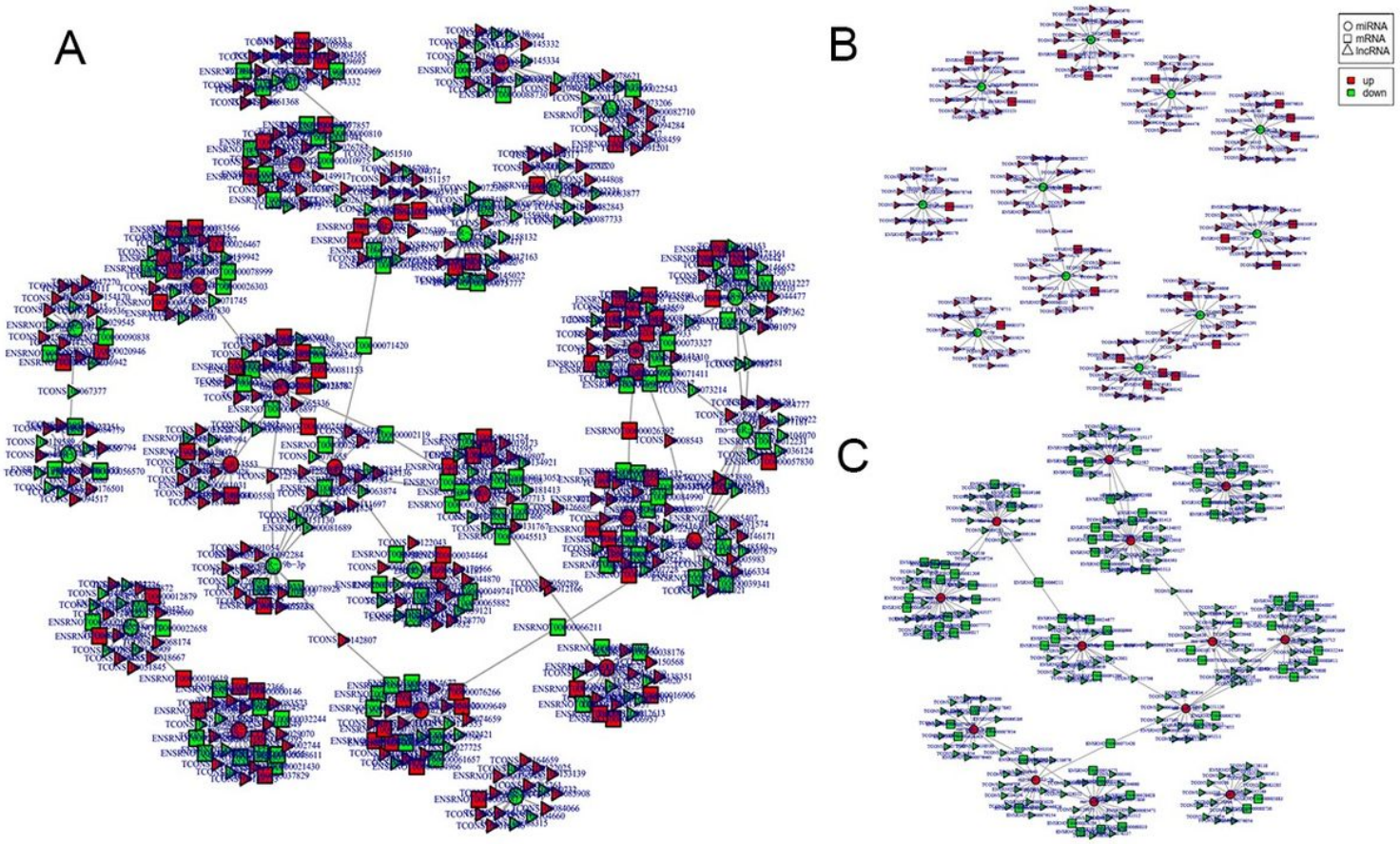

Figure 6

The interactions in the mRNA–lncRNA–miRNA network. Triangle: lncRNAs; Circle: miRNAs; Square: mRNAs. Red: up-regulated; Green: down-regulated. (A) The interactions in all DE mRNAs, lncRNAs and miRNAs. (B) The interactions in up-regulated mRNAs, up-regulated lncRNAs and down-regulated miRNAs. (C) The interactions in up-regulated miRNAs, down-regulated mRNAs and down-regulated lncRNAs.

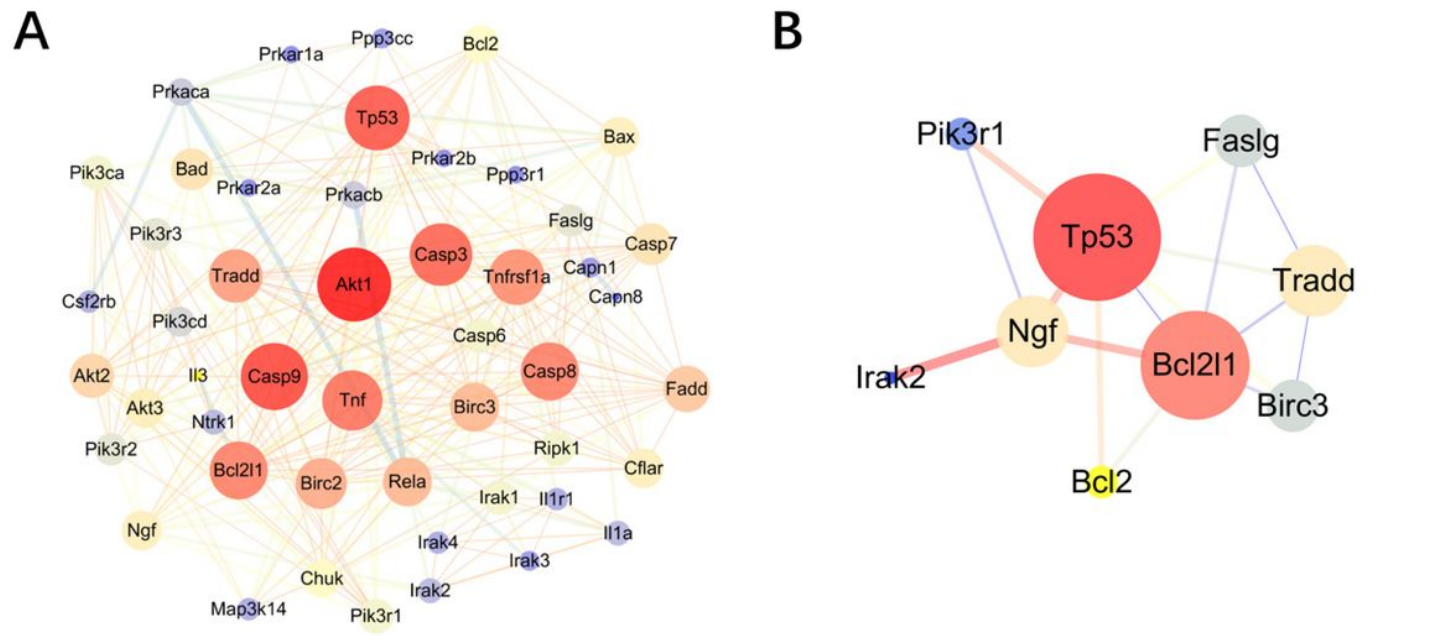

Figure 7

PPI was analyzed using the String. (A) Target genes of DE lncRNAs related KEGG apoptosis pathway. (B) Confluent proteins of DE mRNA genes and target genes of lncRNAs related KEGG apoptosis pathway.

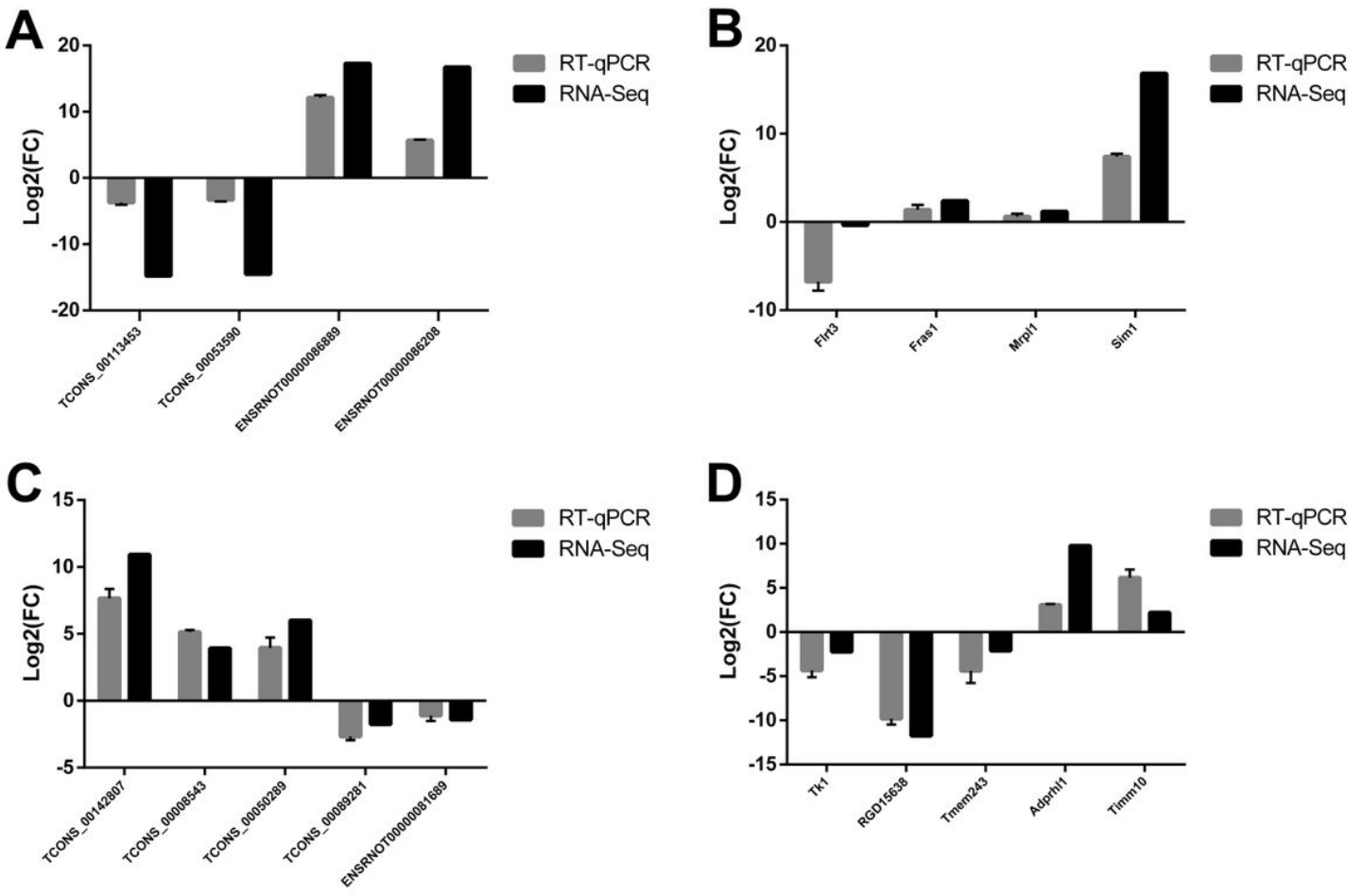

Figure 8

RT-qPCR verification of selected lncRNAs, potential target mRNAs and DE lncRNAs or DE mRNAs closely related to apoptosis exists in the mRNA–lncRNA–miRNA network junction center, compared with transcriptome sequencing. (A) Expressions of the selected lncRNAs validated by RT-qPCR, compared with transcriptome sequencing. (B) Expressions of the selected potential target mRNAs validated by RT-qPCR, compared with transcriptome sequencing. (C) Expressions of the DE lncRNAs validated by RT-qPCR, compared with transcriptome sequencing. (D) Expressions of the DE mRNAs validated by RT-qPCR, compared with transcriptome sequencing.